

# Deep Computerized Adaptive Testing

Jiguang Li\*, Robert Gibbons<sup>†</sup> and Veronika Ročková<sup>‡</sup>

February 27, 2025

## Abstract

Computerized adaptive tests (CATs) play a crucial role in educational assessment and diagnostic screening in behavioral health. Unlike traditional linear tests that administer a fixed set of pre-assembled items, CATs adaptively tailor the test to an examinee’s latent trait level by selecting a smaller subset of items based on their previous responses. Existing CAT frameworks predominantly rely on item response theory (IRT) models with a single latent variable, a choice driven by both conceptual simplicity and computational feasibility. However, many real-world item response datasets exhibit complex, multi-factor structures, limiting the applicability of CATs in broader settings. In this work, we develop a novel CAT system that incorporates multivariate latent traits, building on recent advances in Bayesian sparse multivariate IRT [1]. Our approach leverages direct sampling from the latent factor posterior distributions, significantly accelerating existing information-theoretic item selection criteria by eliminating the need for computationally intensive Markov Chain Monte Carlo (MCMC) simulations. Recognizing the potential suboptimality of existing item selection rules which are often based on myopic one-step-lookahead optimization of some information-theoretic criterion, we propose a double deep Q-learning algorithm to learn an optimal item selection policy. Through simulation and real-data studies, we demonstrate that our approach not only accelerates existing item selection methods but also highlights the potential of reinforcement learning in CATs. Notably, our Q-learning-based strategy consistently achieves the fastest posterior variance reduction, leading to earlier test termination. In finite-horizon settings, it also yields final posterior distributions that more closely approximate the oracle posterior distribution—the posterior that would be obtained if test takers had responded to all items in the item bank.

---

\*Jiguang Li is a 3<sup>rd</sup>-year doctoral student in Econometrics and Statistics at the Booth School of Business of the University of Chicago

<sup>†</sup>Robert Gibbons is the Blum-Reise Professor of Statistics at the University of Chicago

<sup>‡</sup>Veronika Ročková is the Bruce Lindsay Professor of Econometrics and Statistics in the Wallman Society of Fellows

# 1 Introduction

Computerized adaptive testing (CAT) has transformed modern assessment in education and behavioral health by tailoring test content to individual examinees in real time. Unlike traditional linear tests, which present a fixed set of items to all test-takers, CAT dynamically selects questions from a large item bank based on an examinee’s prior responses. This adaptivity enhances both the efficiency and precision of ability estimation by continuously presenting items that are neither too easy nor too difficult [2]. By focusing on items that provide the most information about a test-taker’s latent traits, CAT reduces the number of questions needed to reach an accurate assessment, often enabling earlier test termination without sacrificing measurement accuracy. This efficiency is especially valuable in high-stakes diagnostic settings, such as clinical psychology, where CAT can serve as an alternative to in-person evaluations, helping to expand access to assessments in resource-limited environments [3].

CAT frameworks typically consist of two key components: a psychometric model based on item response theory (IRT) [4] and an online item selection rule that maximizes an information-theoretic criterion (e.g., [5, 6]). Given an observed item response dataset, statisticians first fit an IRT model to estimate item characteristic parameters, which capture properties such as discrimination and difficulty of each item. These parameters provide valuable psychometric insights that guide online item selection for future examinees. The efficiency of a CAT system can be assessed by the number of items required to estimate an examinee’s latent traits with sufficient precision, typically defined as reducing uncertainty below a predetermined threshold.

The psychometric models underlying many CAT frameworks can be overly simplified and inflexible. For practical reasons, most implementations assume a traditional IRT model with a single latent variable, primarily to mitigate the computational challenges of rapid online item selection in high-dimensional, multi-factor latent spaces. However, this assumption is often questionable in real-world item response datasets, such as cognitive assessments in behavioral health [7], where items span multiple domains. As a result, it can lead to biased estimates of item parameters and, consequently, latent trait estimates, ultimately limiting the adaptivity of current CAT systems in many assessment settings. While fitting a multidimensional IRT (MIRT) model is conceptually straightforward, updating high-dimensional latent trait estimates and optimizing item selection criteria in real time remain computationally challenging.

Although numerous item selection rules have been proposed in the CAT literature, they all rely on one-step lookahead greedy optimization of an information-theoretic criterion [8, 9, 10, 6]. For example, the D-optimality criterion selects items that maximize the determinant of the Fisher information matrix evaluated at the current latent trait estimates [8], while the mutual information criterion maximizes entropy reduction in the posterior

distribution [5, 6]. Despite their ease of implementation, these selection rules are inherently myopic and suboptimal, as they fail to account for future decisions. Intuitively, existing methods tend to favor items with high discrimination parameters [11]. However, CAT researchers often recommend reserving highly discriminating items for the later stages of testing to improve efficiency [12, 11]. Integrating this heuristic guidance into existing selection rules, however, remains nontrivial.

To address these critical challenges, we propose a novel deep CAT system that integrates a flexible Bayesian MIRT model with a non-myopic online item selection policy, guided by reinforcement learning (RL) principles [13]. Leveraging recent advancements in Bayesian sparse MIRT [1], our framework seamlessly accommodates multiple latent factors with complex loading structures, while maintaining scalability in both the number of items and factors. For learning the optimal item selection policy, we draw on contemporary RL methodologies [13] and introduce a general double deep Q-learning algorithm [14, 15]. This algorithm trains a deep Q-network offline using only item parameter estimates which is subsequently deployed online to select optimal items based on the current multivariate latent factor posterior distribution.

A primary contribution of our work is the dramatic improvement in computational scalability for existing computerized adaptive testing (CAT) systems, enabling them to adapt more effectively to challenging assessment environments. This rapid online computation is achieved by characterizing the multivariate latent factor posterior distributions as instances of the unified skew-normal distribution [16], which allows for direct and parallel sampling [17, 1, 18]. By circumventing the need for computationally intensive Markov Chain Monte Carlo (MCMC) simulations, our approach facilitates the integration of CATs with arbitrary multidimensional item response theory (MIRT) models. Importantly, this computational advance is not limited to our proposed deep Q-learning framework; it also accelerates existing Bayesian item selection rules, such as those based on Kullback-Leibler (KL) information, including maximizing mutual information [5], as well as any Bayesian procedure requiring sampling from latent factor posterior distributions.

Another critical advancement in our work is the reformulation of computerized adaptive testing (CAT) as a reinforcement learning (RL) problem. This is motivated by the well-documented limitations of greedy approaches in current CAT item selection strategies, which often lead to suboptimal policies [13, 19]. The sequential nature of CAT aligns naturally with deep Q-learning methods, which have demonstrated remarkable success across diverse application domains [14, 20, 21]. However, the intersection of CAT and RL remains largely unexplored. One notable exception is a study by [22], which applies deep Q-learning in adaptive learning systems to select optimal learning materials for students based on their ability estimates. Their simulations demonstrate the effectiveness of Q-learning in assigning three distinct learning materials under a two-factor model. Nevertheless, designing CAT

systems presents unique challenges, as they require both minimal online item selection time and the ability to handle large item banks.

Our work also aligns with the emerging research trend of framing traditional statistical sequential decision-making and adaptive data collection problems as optimal policy learning tasks [23]. In Bayesian adaptive design [24], a dominant strategy involves selecting the next experiment to maximize expected information gain [25]. More recently, [26] demonstrated the effectiveness of deep neural networks in learning non-myopic policies that optimize cumulative information gain across an entire experimental sequence. Similarly, in Bayesian optimization (BO), classical strategies such as expected improvement [27] and upper confidence bound [28] typically employ myopic one-step optimization. To mitigate this limitation, approaches such as Entropy Search (ES) [29] and multi-step lookahead with rollout [30] have shown considerable success in improving long-term performance. By combining the deep Q-learning approach with the flexible Bayesian MIRT framework, our work contributes to these advancements by providing a principled approach to mitigating myopic decision-making in CAT.

The remainder of the paper is organized as follows. Section 2 reformulates the traditional CAT problem as a reinforcement learning task and reviews existing information-theoretic item selection approaches, highlighting their limitations. Section 3 introduces a general strategy for sequentially sampling latent factor posterior distributions under a general MIRT model, eliminating the need for MCMC simulations. We also demonstrate how these techniques can accelerate existing Bayesian item selection methods. Section 4 presents our reinforcement learning approach for optimal item selection, detailing the neural network design and the development of the double Q-learning algorithm. Finally, Section 5 evaluates our method through simulations and real data experiments.

## 2 From One-Step Optimization to Policy Learning

We formally define the problem of designing a computerized adaptive testing (CAT) system from a reinforcement learning (RL) perspective. The development of a CAT system involves two key steps:

- **Offline Calibration:** An item response theory (IRT) model is fitted to a calibrated dataset  $Y \in \mathbb{R}^{N \times J}$  to estimate the item characteristic parameters  $\{\xi_j\}_{j=1}^J$ . Here  $N$  represents the number of examinees, and  $J$  represents the number of items in the item bank.
- **Online Deployment:** Given the estimated item parameters  $\{\xi_j\}_{j=1}^J$ , an item selection algorithm (e.g., maximizing mutual information [5]) is deployed online to adaptively select items for future examinees.

The performance of a CAT system is typically evaluated by the number of items required to estimate an examinee’s latent traits with sufficient precision, often defined as reducing uncertainty below a predetermined threshold. Using the notations defined in Section 2.1, we discuss the existing methods for online item selection in Section 2.2, highlighting the limitations of the one-step optimization greedy approach. We then argue for the need to reframing the traditional CAT problem as an RL problem in Section 2.3 .

## 2.1 Notations and Problem Setups

For the entirety of the paper, we assume the calibration dataset  $Y$  is binary, where each element  $y_{ij}$  represents whether subject  $i$  answered item  $j$  correctly. We consider a general two-parameter MIRT framework with  $K$  latent factors [4]. Let  $B \in \mathbb{R}^{J \times K}$  denote the factor loading matrix, and  $D \in \mathbb{R}^J$  denote the intercept vector. For each examinee  $i$  with multivariate latent trait  $\theta_i \in \mathbb{R}^K$ , the data-generating process for  $y_{ij}$  is given by:

$$y_{ij}|\theta_i, B_j, d_j \sim \text{Bernoulli}(\Phi(B'_j\theta_i + D_j)), \quad (1)$$

where  $B_j$  is the  $j$ -th row of  $B$ ,  $D_j$  is the  $j$ -th entry of  $D$ ,  $\Phi(\cdot)$  represents a standard normal cumulative distribution link function. The item parameters can be compactly expressed as  $\{\xi_j\}_{j=1}^J := \{(B_j, D_j)\}_{j=1}^J$ . We emphasize that this two-parameter MIRT framework is highly general, as it does not impose specific structures on the loading matrix  $B$  or require particular estimation algorithms for the item parameters.

Given the estimated item parameters  $\{\xi_j\}_{j=1}^J$ , the second component of CATs involves designing an adaptive item selection algorithm that tests a future examinee with unobserved latent ability  $\theta \in \mathbb{R}^k$  (not in the calibration set). The sequential nature of the CAT problem, combined with recent advancements in posterior updating for Bayesian MIRT models [1], makes Bayesian approaches particularly appealing. Without loss of generality, we assume a standard zero-mean multivariate Gaussian prior with the identity covariance matrix on  $\theta \sim N(0, \mathbb{I}_K)$ . We further define the following notations during online item selection.

- For any positive integer  $n$ , let  $[n]$  denote all the positive integers no greater than  $n$ . Let  $j \in [J]$  be the index for the items in the item bank.
- Let  $j_t$  denote the index of the item selected at step  $t$  based on an arbitrary item selection rule. Define  $\mathcal{I}_t$  as the set of the first  $t$  administered items, and let  $R_t := [J] \setminus \mathcal{I}_{t-1}$ , the set of available items before the  $t$ -th item is picked.
- We use the shorthand notation  $f(\theta|Y_{1:T})$  to represent the latent factor posterior distributions  $f(\theta|Y_{1:T}, \xi_{1:T})$  after  $T$  items have been selected. Here, the response history is denoted by  $Y_{1:T} := [y_{j_1}, \dots, y_{j_T}]'$ , and the item parameters are given by  $\xi_{1:T} := (B_{1:T}, D_{1:T})$ , where  $B_{1:T} := [B_{j_1}, \dots, B_{j_T}]'$  and  $D_{1:T} := [D_{j_1}, \dots, D_{j_T}]'$ .

At time  $(t+1)$ , the item selection algorithm takes the current posterior  $f(\theta|Y_{1:t})$  as input and outputs the next item selection  $j_{t+1}$ . Suppose this process continues until at time  $T'$ , either when the posterior variance of  $f(\theta|Y_{1:T'})$  falls below a predefined threshold  $\tau^2$ , or when  $T' = H$ , where  $H \leq J$  is the maximum number of items that can be administered. Hence the goal of CATs is to minimize  $T'$  given the estimated item parameters of the item bank.

## 2.2 Reviews of Existing Item Selection Rules

A substantial line of research in computerized adaptive testing (CAT) has focused on item selection strategies derived from optimal experimental design principles. One widely adopted strategy leverages the D-optimality criterion, which selects items to maximize the determinant of the Fisher information matrix evaluated at the current latent trait estimate [8]. This approach prioritizes items that minimize the volume of the confidence ellipsoid around the latent trait estimate. Alternatively, the A-optimality criterion aims to minimize the trace of the asymptotic covariance matrix of the latent trait estimates [9], thereby reducing overall estimation variance.

Another prominent line of research employs Kullback-Leibler (KL) information within a Bayesian framework. Bayesian methods are particularly advantageous in CAT, as they provide a natural statistical framework for updating posterior beliefs about latent traits, thereby enabling more informed and adaptive item selection. Recent work [31] highlights the theoretical and empirical advantages of Bayesian mutual information (MI) over classical criteria such as D-optimality [8] and continuous entropy minimization [32]. These findings underscore the potential of Bayesian CAT algorithms to improve estimation accuracy and testing efficiency. Given that our proposed deep CAT system builds on recent advances in Bayesian MIRT [1], we now review Bayesian item selection rules in detail.

A common Bayesian approach is the KL Expected A Priori (EAP) rule, which selects the  $t$ -th item based on the average KL distance between response distributions on the candidate item at the EAP estimate  $\hat{\theta}_{t-1}$  and random factor  $\theta$  sampled from the posterior distribution  $f(\theta|Y_{1:(t-1)})$  [10]:

$$\arg \max_{j_t \in R_t} K_{j_t}^B(\hat{\theta}_{t-1}) = \arg \max_{j_t \in R_t} \int_{\theta} K_{j_t}(\hat{\theta}_{t-1}; \theta) f(\theta|Y_{1:(t-1)}) d\theta, \quad (2)$$

where

$$\hat{\theta}_{t-1} = \int_{\theta} \theta f(\theta|Y_{1:(t-1)}) d\theta,$$

$$K_{j_t}(\hat{\theta}_{t-1}; \theta) = \mathbb{E} \left[ \log \frac{f(y_{j_t}|\hat{\theta}_{t-1})}{f(y_{j_t}|\theta)} \right] = \sum_{l=0}^1 P(y_{j_t} = l|\hat{\theta}_{t-1}) \log \frac{P(y_{j_t} = l|\hat{\theta}_{t-1})}{P(y_{j_t} = l|\theta)}.$$

Rather than focusing on the KL distance based on the response distributions, the authors in [6] propose the MAX Pos approach by maximizing the KL distance between two subsequent latent factor posteriors  $f(\theta|Y_{1:(t-1)})$  and  $f(\theta|Y_t)$ . Intuitively, this approach prioritizes items that induce the largest shift in the posterior, formalized as:

$$\arg \max_{j_t \in R_t} K_{j_t}^P[f(\theta|Y_{1:(t-1)})] = \arg \max_{j_t \in R_t} \sum_{y_{j_t}=0}^1 f(y_{j_t}|Y_{1:(t-1)}) \int_{\theta} f(\theta|Y_{1:(t-1)}) \log \frac{f(\theta|Y_{1:(t-1)})}{f(\theta|Y_{1:t})} d\theta, \quad (3)$$

where  $f(y_{j_t}|Y_{1:(t-1)})$  represents the posterior predictive probability:

$$f(y_{j_t}|Y_{1:(t-1)}) = \int_{\theta} f(y_{j_t}|\theta) f(\theta|Y_{1:(t-1)}) d\theta. \quad (4)$$

A third Bayesian strategy, the mutual information (MI) approach, maximizes the mutual information between the current posterior distribution and the response distribution of new item  $y_{j_t}$  [5]. Rooted in experimental design theory [33], this method has demonstrated empirical success in CAT [31]. We can also interpret mutual information as the entropy reduction of the current posterior estimation of  $\theta$  after observing new response  $y_{j_t}$ . More formally:

$$\arg \max_{j_t \in R_t} I_M(\theta, y_{j_t}) = \arg \max_{j_t \in R_t} \sum_{y_{j_t}=0}^1 \int_{\theta} f(\theta, y_{j_t}|Y_{1:(t-1)}) \log \frac{f(\theta, y_{j_t}|Y_{1:(t-1)})}{f(\theta|Y_{1:(t-1)}) f(y_{j_t}|Y_{1:(t-1)})} d\theta \quad (5)$$

Although existing item selection rules, whether frequentist or Bayesian, are interpretable and grounded in information theory, they share a common limitation: relying on one-step lookahead optimization without considering future decisions. This limitation motivates us to develop a more principled item selection strategy using reinforcement learning.

## 2.3 Reinforcement Learning Formulation

Traditional item selection rules in CAT, as discussed above, inherently suffer from myopic decision-making, which can lead to suboptimal testing strategies [13, 19]. A more principled approach is to formulate item selection as a reinforcement learning (RL) problem, where the optimal policy is learned using Bellman optimality principles rather than relying on heuristics that ignore long-term planning. The transition from heuristic sequential decision rules to learned optimal policies has shown empirical success in other areas of statistics, such as adaptive experimental design [26, 23] and Bayesian optimization [30].

Beyond addressing myopia, an RL-based formulation provides a direct mechanism to optimize the fundamental objective of CAT: minimizing the number of items required to reach a predefined posterior variance reduction threshold. While existing item selection



rules attempt to achieve this goal indirectly through information-theoretic criteria, such as mutual information, they do not explicitly minimize the number of test items needed to achieve a desired precision level. In contrast, an RL algorithm can be designed to optimize this objective directly, leading to a more efficient and adaptive testing process. Moreover, RL offers greater flexibility in designing reward functions to accommodate specific user needs. For instance, in bifactor MIRT models [34], an assessment may prioritize accurate estimation of the primary factor while operating in a multidimensional latent space (see Section 5.2 for an example). A well-crafted reward function can explicitly guide item selection toward minimizing variance for the primary factor, ensuring that the test adapts to the most relevant dimensions of interest.

We hence proceed to formulate the item selection problem in CAT as a policy learning problem under the reinforcement learning framework. Consider a general finite horizon setting where each examinee can answer at most  $H \leq J$  items, and the CAT algorithm terminates whenever the posterior variance of the factors of the interests is smaller than a certain threshold  $\tau^2$ , or when  $H$  is reached. While  $H$  can be set sufficiently large to make it non-restrictive, it serves as a practical secondary stopping criterion to prevent excessively long tests, and simplifies the policy learning problem. We can then formulate item selection problem as a standard reinforcement learning problem:

- **State Space  $\mathcal{S}$ :** the space of all possible latent factor posteriors

$$\mathcal{S} := \{f(\theta|Y_{1:t}) : t \in \{1, \dots, H\}\}.$$

We may write the state variable at time  $t$  as  $s_t := f(\theta|Y_{1:t})$ , with  $s_0$  defined as the standard multivariate Gaussian prior distribution on  $\theta$ . Observe the state space is discrete and can be exponentially large. Since there are  $J$  items in the item bank and the responses are binary, the total number of possible states is  $\sum_{t=1}^H \binom{J}{t} \cdot 2^t$ .

- **Action space  $\mathcal{A}$ :** the whole action space is  $[J] := \{1, \dots, J\}$ . However, at the  $t$ -th selection time, the action space is  $R_t := [J] \setminus \mathcal{I}_{t-1}$ , since we do not administer the same item twice.
- **Transition Kernel  $\mathcal{P} : \mathcal{S} \times \mathcal{A} \rightarrow \Delta(\mathcal{S})$ ,** where  $\Delta(\mathcal{S})$  is the state of probability distribution over  $\mathcal{S}$ . Observe the transitional kernel in CATs has a very simple structure: conditional on any give state action pair  $(s, a)$ , the next step posterior can only have two distinct outcomes, depending on whether the test taker has answered item  $a$  correctly or not. However, we cannot exactly pinpoint the transition probability, as knowing the probability of answering a given item correctly requires the full knowledge of the multivariate latent trait  $\theta \in \mathbb{R}^K$ , which is unavailable.



- **Reward Function:** To encourage our CAT algorithm to terminate quickly, we minimize the number of items required to achieve the desired precision by assigning a simple 0 – 1 reward structure. In a  $K$ -factor MIRT model, we often prioritize a subset of factors  $\mathcal{K} \in [K]$ , with the test terminating once the posterior variances of all factors in  $\mathcal{K}$  fall below the predefined threshold  $\tau^2$ . Formally, the reward function is defined as

$$R^{(t)}(s_t, a, s_{t+1}) = \begin{cases} -1 & \text{if } V_{t+1} > \tau^2, \\ 0 & \text{otherwise,} \end{cases}$$

where  $V_{t+1} = \max_{k \in \mathcal{K}} \text{Var}(\theta_k | Y_t)$  is the maximum marginal posterior variance among the prioritized factors  $\mathcal{K}$ . This reward structure offers two key advantages: interpretability and computational efficiency. Notably, it simplifies the learning of the state-action value function, as the rewards are always bounded integers within  $[-H, -1]$ . A similar reward formulation has been explored in adaptive learning settings [22].

Rather than following a heuristic decision rule, we focus on learning a policy function  $\pi(s)$ , defined as a mapping from the current posterior distribution  $s_t$ , to a probabilities of selecting each remaining item in  $R_t$ . Given a prior distribution  $s_0 \sim N(0, \mathbb{I}_K)$ , we define its value function under a policy  $\pi(s)$  as

$$v_\pi(s_0) := \mathbb{E}_\pi \left[ \sum_{t=0}^{H-1} \gamma^t R^{(t)}(s_t, \pi(s_t), s_{t+1}) | S_0 = s_0 \right], \quad (6)$$

where  $\gamma \in [0, 1)$  is the discount factor. Our goal is to find an optimal policy  $\pi^*(s)$  which maximizes the the value function

$$\pi^*(s_0) := \operatorname{argmax}_\pi v_\pi(s_0).$$

To facilitate the search for the optimal policy, we introduce the action-value Q function under an arbitrary policy  $\pi$ :

$$Q_\pi(s_0, a) := \mathbb{E}_\pi \left[ \sum_{t=0}^{H-1} \gamma^t R^{(t)}(s_t, \pi(s_t), s_{t+1}) | S_0 = s_0, A_0 = a \right], \quad (7)$$

where action (item)  $a$  is chosen initially. By the Bellman optimality equation [13], we have  $v_{\pi^*}(s_t) = \max_{a \in R_{t+1}} Q_{\pi^*}(s_t, a)$ , so solving for  $\pi^*$  amounts to solving the following Bellman Equation [19]:

$$Q_\pi(s_t, a_t) = \mathbb{E}_\pi [R(s_t, \pi(s_t), s_{t+1})] + \gamma \sum_{s_{t+1} \in \mathcal{S}} \mathcal{P}(s_{t+1} | s_t, a_t) \max_{a_{t+1} \in \mathcal{R}_{t+2}} Q(s', a'). \quad (8)$$

Since the state space grows exponentially and the action space is nontrivial, solving for  $\pi^*$  using traditional dynamic programming approaches like value iteration or tabular Q-learning become intractable [13]. In section 4, we propose a double deep Q-learning approach [14, 15] to approximate the optimal policy.

### 3 Accelerating Item Selection via Direct Sampling

Our proposed deep CAT system builds on recent advances in sparse Bayesian MIRT [1], which eliminates rigid constraints on the factor loading matrix  $B$ . This flexibility makes our approach highly adaptable across diverse item banks and application domains. By adopting a probit link function, the posterior updates for the multivariate latent factors remain tractable under the MIRT model in Equation (1), thereby bypassing the need for computationally expensive MCMC procedures. This substantial computational improvement not only enhances the efficiency of our proposed Q-learning framework, but also accelerates existing CAT systems. In Section 3.1, we demonstrate how our method improves the efficiency of common Bayesian item selection rules, while in Section 3.3, we extend our approach to fully Bayesian online computation, incorporating uncertainty in the item parameters.

A key contribution of our work is demonstrating that direct sampling from the latent factor posterior distributions during CAT is computationally tractable. This is achieved by repeatedly applying the E-step of the PXL-EM algorithm for estimating MIRT models, as introduced in [1]. Specifically, [1] shows that, conditional on the MIRT item parameters during the E-step, the latent factor posterior distributions belong to an instance of the unified skew-normal distribution:

**Definition 3.1.** Let  $\Phi_J\{V; \Sigma\}$  represent the cumulative distribution functions of a  $J$ -dimensional multivariate Gaussian distribution  $N_J(0_J, \Sigma)$  evaluated at vector  $V$ . A  $K$ -dimensional random vector  $z \sim \text{SUN}_{K,J}(\xi, \Omega, \Delta, \gamma, \Gamma)$  has the **unified skew-normal** distribution if it has the probability density function:

$$\phi_K(z - \xi; \Omega) \frac{\Phi_J\{\gamma + \Delta^T \bar{\Omega}^{-1} \omega^{-1}(z - \xi); \Gamma - \Delta^T \bar{\Omega}^{-1} \Delta\}}{\Phi_J(\gamma; \Gamma)}.$$

Here,  $\phi_K(z - \xi; \Omega)$  is the density of a  $K$ -dimensional multivariate Gaussian with expectation  $\xi = (\xi_1, \dots, \xi_K)'$ , and a  $K$  by  $K$  covariance matrix  $\Omega = \omega \bar{\Omega} \omega$ , where  $\bar{\Omega}$  is the correlation matrix and  $\omega$  is a diagonal matrix with the square roots of the diagonal elements of  $\Omega$  in its diagonal.  $\Delta$  is a  $K$  by  $J$  matrix that determines the skewness of the distribution, and  $\gamma \in \mathbb{R}^J$  control the flexibility in departures from normality.

In addition, the  $(K + J) \times (K + J)$  matrix  $\Omega^*$ , having blocks  $\Omega_{[11]}^* = \Gamma, \Omega_{[22]}^* = \bar{\Omega}$  and  $\Omega_{[21]}^* = \Omega_{[12]}^{*'} = \Delta$ , needs to be a full-rank correlation matrix.

Suppose an arbitrary CAT item selection algorithm has already selected  $T$  items with item parameters  $\xi_{1:T} = (B_{1:T}, D_{1:T})$ , where  $B_t := [B_{j_1}, \dots, B_{j_T}]'$  and  $D_{1:T} := [D_{j_1}, \dots, D_{j_T}]'$ . Then, a direct application of Theorem 4.2 in [1] would yield the following result:

**Theorem 3.2.** *Consider a  $K$ -factor CAT item selection procedure after selecting  $T$  items, with  $N(0, \mathbb{I}_K)$  prior placed on the test taker's latent trait  $\theta$ . If  $Y_{1:T} = (y_{j_1}, \dots, y_{j_T})' \in \mathbb{R}^t$  is conditionally independent binary response data from the two-parameter probit MIRT model defined in (1), then*

$$(\theta \mid Y_{1:T}, B_{1:T}, D_{1:T}) \sim \text{SUN}_{K,T}(\xi_{\text{post}}, \Omega_{\text{post}}, \Delta_{\text{post}}, \gamma_{\text{post}}, \Gamma_{\text{post}}),$$

with posterior parameters

$$\begin{aligned} \xi_{\text{post}} &= 0_K, \quad \Omega_{\text{post}} = \mathbb{I}_K, \quad \Delta_{\text{post}} = D_1' D_3^{-1}, \\ \gamma_{\text{post}} &= D_3^{-1} D_2, \quad \Gamma_{\text{post}} = D_3^{-1} (D_1 D_1' + \mathbb{I}_t) D_3^{-1}, \end{aligned}$$

where  $D_1 = \text{diag}(2y_{j_1} - 1, \dots, 2y_{j_T} - 1) B_{1:T}$  and  $D_2 = \text{diag}(2y_{j_1} - 1, \dots, 2y_{j_T} - 1) D_{1:T}$ . The matrix  $D_3$  is a  $T$  by  $T$  diagonal matrix, where the  $(t, t)$ -th entry is  $(\|B_{t,T}\|_2^2 + 1)^{\frac{1}{2}}$ , with  $B_{t,T}$  representing the  $t$ -th row of  $B_{1:T}$ .

As demonstrated in [16], the distribution of an arbitrary unified skew normal distribution  $\theta \sim \text{SUN}_{K,T}(\xi, \Omega, \Delta, \gamma, \Gamma)$  has a stochastic representation as a linear combination of a  $K$ -dimensional multivariate normal random variable  $V_0$ , and a  $T$ -dimensional truncated multivariate normal random variable  $V_{1,-\gamma}$  as follows:

$$\theta \stackrel{d}{=} \xi + \omega(V_0 + \Delta \Gamma^{-1} V_{1,-\gamma}), \quad (9)$$

where  $V_0 \sim N(0, \bar{\Omega} - \Delta \Gamma^{-1} \Delta') \in \mathbb{R}^K$  and  $V_{1,-\gamma}$  is obtained by component-wise truncation below  $-\gamma$  of a variate  $N(0, \Gamma) \in \mathbb{R}^T$ .

Based on Theorem 3.2 and equation (9), sampling from latent factor posterior distribution  $f(\theta \mid Y_{1:T})$  requires two independent steps: sampling from a  $K$ -dimensional multivariate normal distribution, and a  $T$ -dimensional multivariate truncated normal distribution. As a result, the direct sampling approach scales efficiently with the number of factors  $K$ , since generating samples from  $K$ -dimensional multivariate normal distributions is trivial. Moreover, in CAT settings, the test is typically terminated early, meaning  $T$  remains relatively small. When  $T$  is moderate (e.g.,  $T < 1,000$ , which is always the case for CATs), sampling from the truncated multivariate normal distribution remains computationally efficient using the minimax tilting method of Botev [18].

Theorem 3.2 plays a central role in our proposed deep Q-learning algorithm, as it fully characterizes the latent factor posterior distribution  $f(\theta \mid Y_{1:T})$ , enabling parametrization of the state variable  $s_T$ , which serves as an input to the Q-network illustrated in Section 4.1.

Furthermore, this result significantly accelerates existing CAT systems, a key contribution that will be discussed in the remainder of this section.

### 3.1 Accelerating Existing Rules

We demonstrate how Theorem 3.2 can be applied to accelerate all existing Bayesian item selection rules in Section 2.2. By leveraging the fact that we can now efficiently obtain i.i.d. samples from the latent factor posterior distribution  $f(\theta|Y_{1:t})$  for any  $t \in [H]$  as an instance of the unified skew-normal distribution, we eliminate the need for traditional Markov Chain Monte Carlo (MCMC) methods. Unlike MCMC, our approach avoids additional mixing time requirements and can be easily parallelized.

For example, in computing the KL-EAP item selection rule defined in Equation (2), we can directly sample from  $f(\theta|Y_{1:(t-1)})$  and evaluate the integral via Monte-Carlo integration. Since the EAP estimate  $\hat{\theta}_{t-1}$  remains fixed at time step  $t$ , it only needs to be computed once at the beginning using the same set of posterior samples. Similarly, evaluating the KL information term  $K_{j_t}(\hat{\theta}_{t-1}; \theta)$  for each posterior sample  $\theta \in f(\theta|Y_{1:(t-1)})$  is trivial, as probability evaluations in the two-parameter probit MIRT model are straightforward.

To compute the MAX-Pos item selection rule defined in equation (3), we first obtain i.i.d. samples from the posterior distribution  $f(\theta|Y_{1:(t-1)})$ , enabling the computation of posterior predictive probabilities in Equation (4) via Monte-Carlo integration. However, the computation of KL information may seem daunting, as the ratio of two pdf functions  $\frac{f(\theta|Y_{1:(t-1)})}{f(\theta|Y_{1:t})}$  of the unified-skew normal distribution is extremely difficult to evaluate. To address this, we leverage the conditional independence assumption of the MIRT model. Suppose  $(t-1)$  items have already been selected, and recall  $y_{j_t}$  represents the binary response for item  $j_t$ , should it be selected at time  $t$ . Then, by the conditional independence, we can express the joint distribution of  $(\theta, y_{j_t})$  as

$$f(\theta, y_{j_t}|Y_{1:(t-1)}) = f(\theta|Y_{1:(t-1)}, y_{j_t})f(y_{j_t}|Y_{1:(t-1)}) = f(y_{j_t}|\theta)f(\theta|Y_{1:(t-1)}). \quad (10)$$

Using Equation (10), we rewrite the KL information term in Equation (3) as:

$$\begin{aligned} \int f(\theta|Y_{1:(t-1)}) \log \frac{f(\theta|Y_{1:(t-1)})}{f(\theta|Y_{1:(t-1)}, y_{j_t})} d\theta &= \int f(\theta|Y_{1:(t-1)}) \log \frac{f(\theta|Y_{1:(t-1)})f(y_{j_t}|Y_{1:(t-1)})}{f(\theta, y_{j_t}|Y_{1:(t-1)})} d\theta \\ &= \int f(\theta|Y_{1:(t-1)}) \log \frac{f(y_{j_t}|\theta)}{f(y_{j_t}|Y_{1:(t-1)})} d\theta. \end{aligned}$$

Since  $f(y_{j_t}|Y_{1:(t-1)})$  has already been computed, and  $f(y_{j_t}|\theta)$  can be easily computed for each  $\theta \sim f(\theta|Y_{1:(t-1)})$ , the online-computation of MAX-POS remains efficient.

Although the mutual information selection rule defined in Equation (5) has demonstrated strong empirical performance [31], its computational complexity remains a signif-

icant challenge. By applying the conditional independence property in Equation (10), we can rewrite mutual information as

$$\arg \max_{j_t \in R_t} I_M(\theta, y_{j_t}) = \arg \max_{j_t \in R_t} \sum_{y_{j_t}=0}^1 f(y_{j_t}|Y_{1:(t-1)}) \int_{\theta} f(\theta|Y_{1:(t-1)}, y_{j_t}) \log \frac{f(y_{j_t}|\theta)}{f(y_{j_t}|Y_{1:(t-1)})} d\theta \quad (11)$$

This formulation reveals that maximizing mutual information is structurally similar to MAX-Pos, as both involve KL divergence between subsequent posterior distributions, but in reverse order. While Monte Carlo integration enables a straightforward evaluation of Equation (11), its computational burden is substantially higher. Unlike MAX-Pos, where sampling is performed from the current posterior  $f(\theta|Y_{1:(t-1)})$ , mutual information requires sampling from future posteriors  $f(\theta|Y_{1:(t-1)}, y_{j_t})$ . Since each candidate item  $j_t \in R_t$  has two possible outcomes ( $y_{j_t} = 0$  or  $y_{j_t} = 1$ ), evaluating equation (11) requires obtaining samples from  $|R_t| \times 2$  distinct posterior distributions. Even if sampling each individual posterior is computationally efficient, this approach becomes impractical for large item banks.

We hence propose a new approach to dramatically accelerate the computation of the mutual information quantity using the idea of importance sampling and resampling [35]. Rather than explicitly sampling the future posterior  $f(\theta|Y_{1:(t-1)}, y_{j_t})$  for each  $j_t \in R_t$  and  $y_{j_t} \in \{0, 1\}$ , we can simply sample from the current posterior  $f(\theta|Y_{1:(t-1)})$  once, and then perform proper reweighing. Under our two-parameter probit MIRT framework, let  $p(\theta)$  be the prior on the latent factors  $\theta$ ,  $l_1(\theta)$  be the current data likelihood, and  $l_2(\theta)$  denote the future data likelihood after observing test taker answering an item  $j_t \in R_t$ . We have the future posterior density as below:

$$\begin{aligned} f(\theta|Y_{1:(t-1)}, y_{j_t}) &\propto l_2(\theta)p(\theta) \propto \frac{l_2(\theta)p(\theta)}{l_1(\theta)p(\theta)} f(\theta|Y_{1:(t-1)}) \\ &= \Phi(B'_{j_t}\theta + d_{j_t})^{y_{j_t}} (1 - \Phi(B'_{j_t}\theta + d_{j_t}))^{1-y_{j_t}} f(\theta|Y_{1:(t-1)}). \end{aligned} \quad (12)$$

Equation (12) suggests we can generate samples from  $f(\theta|Y_{1:(t-1)}, y_{j_t})$  reweighing and resampling from the current posterior samples  $f(\theta|Y_{1:(t-1)})$ . Specifically, given a sufficient large set of posterior samples  $(\theta_1, \dots, \theta_M) \sim f(\theta|Y_{1:(t-1)})$ , we assign distinct weights for each sample  $m \in [M]$  and future item  $j_t \in R_t$ :

$$q_m = \frac{w_m}{\sum_{i=1}^M w_i}, \quad \text{where } w_i = \Phi(B'_{j_t}\theta_i + d_{j_t})^{y_{j_t}} (1 - \Phi(B'_{j_t}\theta_i + d_{j_t}))^{1-y_{j_t}}.$$

To sample from  $f(\theta|Y_{1:(t-1)}, y_{j_t})$ , we then draw from the discrete distribution over  $(\theta_1, \dots, \theta_M)$ , placing weight  $q_m$  on  $\theta_m$ . This approach eliminates the need to sample from  $|R_t| \times 2$  distinct posteriors directly, further accelerating mutual information computation and making it scalable for large item banks.

### 3.2 Maximize Prediction Variances

We propose a new heuristic item selection rule that selects items with the highest predictive variance based on the current posterior estimates. Formally, write  $c_{j_t} := f(y_{j_t} | Y_{1:(t-1)})$  as defined in (4), and consider the following criterion:

$$\operatorname{argmax}_{j_t \in R_t} \int_{\theta} (\Phi(B'_{j_t} \theta + d_{j_t}) - c_{j_t})^2 f(\theta | Y_{1:(t-1)}) d\theta. \quad (13)$$

This rule selects the item  $j_t$  that maximizes the variance of the predictive means, weighted by the current posterior  $f(\theta | Y_{1:(t-1)})$ . Intuitively, selecting items where examinee’s responses are highly uncertain is advantageous, as administering items with predictable outcomes may lead to inefficient test adaptation.

More formally, in Appendix A, we establish a connection between this selection rule and the mutual information criterion, showing that both favor items with high prediction uncertainty. Computationally, our method avoids the need for posterior reweighting and log transformations, significantly reducing computational overhead. In both simulations and real-data experiments, our proposed selection rule achieves comparable performance to mutual information-based selection while requiring substantially less computation time.

### 3.3 Fully Bayesian Item Selections

Another key advantage of our direct sampling approach is its ability to enable fully Bayesian item selection. Since Section 2, we have assumed that the item bank is well-calibrated, allowing the factor loading matrix  $B$  and the intercept  $D$  to be treated as fixed. This assumption is reasonable when large item response datasets are available, as item parameters can be reliably estimated from the data. While this is a prevailing assumption in the literature, it is important to acknowledge that it can lead to overly optimistic estimates of the uncertainties in the multidimensional latent traits. Since underestimating uncertainty is particularly risky in high-stakes testing, it is essential to account for uncertainty in item parameter estimation.

A fully Bayesian framework offers a principled way to incorporate this uncertainty by integrating over the joint posterior of item parameters and latent traits. However, performing this integration in online item selection has long been considered intractable, limiting its practical adoption. Notably, [36] introduced an efficient MCMC method for unidimensional item response theory (IRT) models, enabling fast online item selection in a fully Bayesian manner.

Our direct sampling approach extends fully Bayesian item selection to multivariate IRT models while avoiding the computational bottlenecks of MCMC. To illustrate, we consider the mutual information criterion in (11). Given an observed item response data

$Y$ , Bayesian inference typically involves obtaining posterior samples of item parameters  $\{\xi^{(m)}\}_{m=1}^M$ , where  $\xi^{(m)} := (B^{(m)}, D^{(m)})$ . The mutual information criterion in Equation (11) requires computing the posterior predictive probability:

$$f(y_{jt}|Y_{1:(t-1)}) = \int_{\xi} \int_{\theta} f(y_{jt}|\theta) f(\theta|\xi, Y_{1:(t-1)}) d\theta d\xi. \quad (14)$$

Similarly, the KL divergence term in Equation 5 must integrate out nuisance item parameters  $\xi$ :

$$\int_{\xi} \int_{\theta} f(\theta|Y_{1:(t-1)}, y_{jt}, \xi) \log \frac{f(y_{jt}|\theta)}{f(y_{jt}|Y_{1:(t-1)})} d\theta d\xi. \quad (15)$$

The key advantage of our approach is that it allows direct sampling from  $f(\theta|Y_{1:(t-1)}, y_{jt}, \xi^{(m)})$  for any binary vector history  $Y_{1:(t-1)}$  and posterior item parameter sample  $\xi^{(m)}$  in parallel, by leveraging Theorem 3.2. As a result, Equations (14) and (15) become computationally feasible via Monte Carlo integration.

In contrast, a standard MCMC approach requires constructing  $M$  independent Markov chains, each targeting  $f(\theta|Y_{1:(t-1)}, y_{jt}, \xi^{(m)})$ , with sampling only possible after all chains have reached convergence. This introduces a significant computational burden, making MCMC impractical for real-time item selection. Our direct sampling method eliminates this bottleneck, offering an efficient and scalable solution for fully Bayesian adaptive testing. Although our primary focus is not on fully Bayesian item selection, we demonstrate the computational efficiency of our direct sampling approach in Appendix B through an online item selection experiment on a nontrivial three-factor, 150-item simulation.

## 4 Learning Optimal Item Selection Policy

In Section 2.3, we highlight the necessity of transforming the one-step-lookahead optimization of heuristic information-theoretic criteria into a more principled RL-based item selection policy. An RL approach addresses the myopic nature of these selection rules, enables a more flexible reward structure, and directly minimizes the number of items required for performing online adaptive testing. Learning the optimal item selection policy essentially boils down to solving the Bellman equation in (8). Although the summation in (8) includes only two terms based on the examinee’s binary response, solving it becomes quickly intractable for large size of item pool  $J$  and long horizon  $H$ . Since the transition kernel  $\mathcal{P}$  is unknown, and the state space  $\mathcal{S}$  is exponentially large, a natural solution is to build a deep neural network to approximate the optimal action-value function  $Q^*(s, a)$ .

We therefore propose a novel double Q-learning algorithm [14, 15] to learn optimal policies for CAT online item selection. The algorithm trains a deep neural network offline using item parameters estimated from an arbitrary two-parameter MIRT estimation algorithm.



During online item selection, the neural network takes the current state variable (posterior distribution)  $s_t := f(\theta|Y_{1:t})$  as input and outputs the item selection for step  $(t + 1)$ . We describe the neural network architecture in Section 4.1 and the double deep Q-learning algorithm in Section 4.2.

## 4.1 Deep Q-learning Neural Network Design

A potential reason why a deep reinforcement learning approach has not been proposed in the CAT literature is due to the ambiguity arising from unidentified latent factor distributions. However, by Theorem 3.2, it is straightforward to compactly parametrize the posterior distribution  $s_t := f(\theta|Y_{1:t})$  at each time step  $t$  using the parameters  $D_1 \in \mathbb{R}^{t \times K}$ ,  $D_2 \in \mathbb{R}^t$ , and  $\text{diag}(D_3) \in \mathbb{R}^t$ , where  $\text{diag}(D_3)$  represents the diagonal vector of  $D_3$ . Rather than feeding the entire response history and item parameters to the neural network, this structured and compact representation eliminates the ambiguity in posterior updates, facilitating the integration of deep reinforcement learning into CAT frameworks.

Define the collection of the posterior parameters  $\tilde{\xi}_t := \{(D_{1h}, D_{2h}, D_{3h})\}_{h=1}^t$ , where  $D_{1h}$  is the  $h$ -th row of  $D_1$ ,  $D_{2h}$  is the  $h$ -th element of  $D_2$ , and  $D_{3h}$  is the  $h$ -th elements in the diagonal of  $D_3$ . Observe that the size of the posterior parameters  $\tilde{\xi}_t$  grows over time, and permuting the tuples  $(D_{1h}, D_{2h}, D_{3h})$  within  $\tilde{\xi}_t$  still describes the same posterior due to exchangeability. This suggests we have to design a neural network that can take inputs of growing size, and can provide output that is permutation invariant of the inputs. One potential solution to implementing such feature is to consider the idea of weight sharing, which has also recently been adapted in the Bayesian experimental design literature [26]: Let  $\phi_1$  denote the function that maps each tuple  $(D_{1h}, D_{2h}, D_{3h}) \in \mathbb{R}^{K+2}$  into the  $L_1$ -dimensional feature space, and we consider the encoder  $g_1$  as follows:

$$g_1(\tilde{\xi}_t) := \sum_{h=1}^t \phi_1((D_{1h}, D_{2h}, D_{3h})). \quad (16)$$

Observe the encoder  $g_1(\cdot)$  is capable of handling growing number of inputs, and will produce the same output regardless of the order of the tuples  $(D_{1h}, D_{2h}, D_{3h})$  as desired. Although the form of  $g_1$  may look restrictive, any function  $f(\cdot)$  operating on a countable set can be decomposed into the form  $\rho \circ g_1(\cdot)$ , where  $\rho(\cdot)$  is a suitable transformation that can be learned from another neural network (see Theorem 2 of [37]).

In principle, the network design  $\rho \circ g_1(\cdot)$ , coupled with the Q-learning algorithm is sufficient to learn the optimal policy, and can be deployed offline with significantly less computational cost compared to the online item selection rules discussed in Section 2.2, since it does not either sampling or optimization. However, to enhance learning efficiency, we advocate for augmenting the current input space  $\tilde{\xi}_t$  with a matrix of prediction quartiles

$\Psi_t \in \mathbb{R}^{J \times Q}$ , where each row contains a vector of quantiles of the predictive mean distribution for item  $j$ . The distribution of the prediction mean can be formed by drawing samples  $\theta_1, \dots, \theta_M \sim f(\theta|Y_{1:t})$  as described in Section 3, and then computing the quantiles of the prediction samples  $\{\Phi(B'_j\theta_i + d_j)\}_{i=1}^M$  for each item  $j$ . Since sampling from  $f(\theta|Y_{1:t})$  only needs to be done once, computing the matrix  $\Psi_t$  online is computationally efficient.

The motivation for augmenting the input space with  $\Psi_t$  is to provide the neural network with additional contextual information, enabling it to better model the item bank beyond what is captured by the current posterior parameters. Most heuristic item selection rules incorporate some measure of item prediction uncertainty. For instance, it can be shown that the Bayesian mutual information criterion prioritizes items that maximize the expected KL divergence from their posterior predictive mean, as illustrated in Appendix A. However, there is no fundamental reason to assume that KL divergence or squared prediction error from the mean is the most effective way to utilize prediction distributions. By incorporating the full predictive distribution through  $\Psi_t$ , the neural network has the capacity to extract more nuanced patterns, potentially leading to more efficient and adaptive item selection policies. Additionally,  $\Psi_t$  also serves to discourage the network from selecting previously administered items, as their prediction uncertainties are minimal.

In summary, to select the  $(t+1)$ -th item, our proposed neural net takes two inputs: the posterior parameters  $\tilde{\xi}_t$  and the prediction matrix  $\Psi_t$ , and outputs the selected item. Let  $\phi_1$  represent the network component defined in equation (16),  $\phi_2$  the component processing the matrix  $\Psi_t \in \mathbb{R}^{J \times Q}$ , and  $\phi_3$  the hidden layers that maps the concatenated feature space from  $\phi_1$  and  $\phi_2$  to a  $J$ -dimensional logits vector. Denoting the final policy network as  $\pi_\phi$ , our proposed network selects the item corresponding the maximum value of the following softmax function:

$$\pi_\phi(\tilde{\xi}_t, \Psi_t) := \text{Softmax} \left\{ \phi_3(g_1(\tilde{\xi}_t), \phi_2(\Psi_t)) \right\}.$$

## 4.2 Double Deep Q-Learning for CAT

The standard Q-learning algorithm often overestimates Q-values because the Q-network selects actions based on maximization operations, which are then used in network evaluation during training. To address this issue, we adopt the Double Q-learning approach [15], which uses a primary network to select the best action and a separate target network to evaluate it. This separation results in more accurate Q-value approximations and leads to a more stable training process.

Our proposed algorithm is presented in Algorithm table 1. Note that for Q-learning to converge, it is essential to adopt an  $\epsilon$ -greedy policy, where the network makes random item selections with probability  $\epsilon$  and gradually decreases  $\epsilon$  over the course of training. For simplicity, the state variable  $s_t$  in Algorithm 1 is a compact representation of  $(\tilde{\xi}_t, \Psi_t)$  defined in Section 4.1. In practice, we can terminate the training process when both the rewards

and the validation loss stabilize, indicating that the neural network has well approximated the optimal policy.

---

**Algorithm 1:** Double Q-Learning Algorithm for Bayesian CAT

---

**Input** : Total Episodes  $E$ ,  $\epsilon \in [\underline{\epsilon}, \bar{\epsilon}]$  with  $\epsilon^{(0)} = \bar{\epsilon}$ , buffer  $\mathcal{H}$ , target network update frequency  $T$ , batch size  $M$ .

**Output** : Learned Q-network  $Q^A$  for item selection.

**Model parameters:** Primary Q-network  $Q^A$ , target Q-network  $Q^B$ .  
Initialize primary Q-network  $Q^A$  and target Q-network  $Q^B$ , with weights  $w_0^A = w_0^B$ ;

**for**  $i = 1$  **to**  $E$  **do**

Draw  $\theta_i$  from  $N(0, I_k)$ ;

Set initial state  $s_0 := N(0, I_k)$  and available item set  $R_0 = \{1, \dots, J\}$ ;

**for**  $t = 0$  **to**  $H$  **do**

Select action  $a_t$  using  $\epsilon$ -greedy policy:

$$a_t = \begin{cases} \text{Random Selection} & \text{with probability } \epsilon^{(t)} \\ \arg \max_{a \in R_t} \hat{Q}^A(s_t, a) & \text{otherwise.} \end{cases}$$

Observe response  $y_t$ ;

Update available item set  $R_{t+1} = R_t \setminus a_t$ ;

Obtain new state  $s_{t+1}$  and compute reward  $r_t$ ;

**if**  $r_t = 0$  **then**

| Break and proceed to the next episode;

**end**

Store transition  $H_{i,t} := (s_t, a_t, r_t, R_t, s_{t+1})$  into buffer  $\mathcal{H}$ ;

**if**  $|\mathcal{H}| > \text{batch size } M$  **then**

Randomly sample  $M$  transitions  $\{H_{i,t}\}_{j=1}^M$  from  $\mathcal{H}$ ;

Compute  $a_j = \arg \max_{a \in R_j} \hat{Q}^A(s_t, a)$ ;

Compute target:

$$y^{(j)} = \begin{cases} -1 & r_j = 0 \\ -1 + \gamma \hat{Q}^B(s'_j, a_j) & \text{otherwise.} \end{cases}$$

Perform batch gradient descent on loss:  $\sum_{j=1}^M (y^{(j)} - \hat{Q}^A(s_j, a_j))^2$ ;

**end**

Decrease  $\epsilon^{(t)}$  if  $\epsilon^{(t)} \geq \underline{\epsilon}$ ;

**end**

Update target network  $Q^B$  such that  $w_t^A = w_t^B$  if  $i$  is a multiple of  $T$ ;

**end**

---

### 4.3 Remark on the Choice of Reward Functions

If the objective of CAT extends beyond early test termination with rapid posterior variance reduction, alternative reward functions can be considered, deviating from the formulation

in Section 2.3. For instance, practitioners might aim to maximize cumulative variance reduction over  $H$  steps, rather than prioritizing dynamic termination. However, the simple 0-1 reward structure offers several advantages. It is interpretable, has demonstrated effectiveness in related problems such as deep adaptive learning [22], and ensures that the cumulative reward remains constrained to integer values between  $-H$  and  $-1$ . This bounded structure simplifies the prediction of cumulative rewards from the current state using the neural network, thereby stabilizing training in our double Q-learning algorithm.

Additionally, for certain reward functions, the advantages of applying the reinforcement learning approach may be minimal compared to the greedy optimization approach that simply maximizes the next-step reward, such as the traditional CAT selection algorithms discussed in Section 2.2. In [38], the authors demonstrate that for a class of dynamic optimization problems known as the stochastic depletion problem, the expected rewards generated by a myopic policy are at least 50% of those produced by the optimal policy. For the CAT problem, we can prove similar results under specific reward structures. To illustrate this, we extend the original state space  $\mathcal{S}$  with an additional time variable as  $\bar{\mathcal{S}} = \{(f(\theta | Y_{1:t}), t) : t \in [H]\}$ . Let  $\pi^*(\bar{s})$  represent the optimal policy, and  $\pi^m(\bar{s})$  the myopic policy that maximizes the next-step expected reward. Define the mapping  $\hat{G}_{y_a} : \bar{s} \rightarrow \bar{s}'$  as the posterior update after observing the binary response random variable  $y_a$ , with an incremented time step, where  $\bar{s} = (f(\theta|Y_{1:t}), t)$  and  $\bar{s}' = (f(\theta|Y_{1:t}, y_a), t + 1)$ . Similarly, define  $\tilde{G}_{y_a} : \bar{s} \rightarrow \bar{s}'$  as the posterior update after observing  $y_a$  while keeping the time step fixed, where  $\bar{s} = (f(\theta|Y_{1:t}), t)$  and  $\bar{s}' = (f(\theta|Y_{1:t}, y_a), t)$ .

To show the near optimality of the myopic policy, the authors in [38] make two key assumptions termed as “value function monotonicity” and “immediate rewards”. Recall the value function and the action-value Q-function as defined in (6) and (7) respectively. These assumptions can be adopted to the CAT settings as follows:

- **Immediate Rewards:** for any time stamp  $t < H$ , suppose the myopic policy  $\pi^m$  chooses item  $a$ , then we must have

$$V_{\pi^*}(\bar{s}) \leq E[R(\bar{s}, a, \bar{s}')] + V_{\pi^*}(\tilde{G}_{y_a}(\bar{s})). \quad (17)$$

Essentially, the property says given a free item (without increasing the time step) chosen by the myopic policy would not deteriorate the optimal rewards.

- **Value Function Monotonicity:** for any time stamp  $t < H$ , suppose the optimal policy would choose item  $a_1$  yet the myopic policy would chooses item  $a_2$ , then we must have

$$V_{\pi^*}(\hat{G}_{y_{a_2}}(\tilde{G}_{y_{a_1}}(\bar{s}))) \leq V_{\pi^*}(\hat{G}_{y_{a_2}}(\bar{s})) \quad (18)$$

Note both sides of inequality refer to the optimal value function evaluated at the posterior distribution at time step  $t + 1$ .

In Theorem 4.1, we establish that a reinforcement learning approach to CAT cannot significantly outperform the one-step-lookahead greedy policy when the reward function satisfies the two assumptions outlined above. The proof is provided in Appendix C.

**Theorem 4.1.** *Consider the finite horizon CAT problem with  $H$  steps. Suppose the assumptions of immediate rewards in (17) and value function monotonicity in (18) hold, we have  $V_{\pi^*}(\bar{s}) \leq 2V_{\pi^m}(\bar{s})$  for all  $\bar{s} \in \bar{\mathcal{S}}$ .*

Theorem 4.1 can be interpreted as a negative result for the reinforcement learning approach when the problem structure and reward functions satisfy the assumptions of immediate rewards and value function monotonicity, as it suggests that a simple myopic policy serves as a 2-approximation to the optimal policy. However, it also highlights the advantage of the simple 0-1 reward function as the value function monotonicity is unlikely to hold, rendering the theorem inapplicable. Specifically, the expected posterior variance of  $\hat{G}_{y_{a_2}}(\tilde{G}_{y_{a_1}}(\bar{s}))$  is expected to be smaller than that of  $\hat{G}_{y_{a_2}}(\bar{s})$ . Consequently, fewer items are expected for the posterior  $\hat{G}_{y_{a_2}}(\tilde{G}_{y_{a_1}}(\bar{s}))$  to reach the minimum variance threshold, which implies  $V_{\pi^*}(\hat{G}_{y_{a_2}}(\tilde{G}_{y_{a_1}}(\bar{s}))) \geq V_{\pi^*}(\hat{G}_{y_{a_2}}(\bar{s}))$ .

In contrast, if we set the reward as maximizing the cumulative variance reduction over  $H$  steps, rather than the 0 – 1 reward, the value function monotonicity assumption is more likely to hold. This is because cumulative variance reduction starting from a posterior with smaller variance is expected to be less than that from a posterior with larger variance, given the same remaining item budgets. We may also expect the immediate reward property to hold, as the right hand side of equation (17) has an additional item in the budget, and the expected variance reduction is nonnegative. Thus, Theorem 4.1 provides valuable guidance in avoiding reward structures where the reinforcement learning approach may offer limited advantages.

## 5 Experiments

We evaluate the effectiveness of our deep CAT system through both simulation and real-data experiments, comparing its performance against existing benchmarks across the following three criteria:

1. **Termination Efficiency:** the primary objective of CAT is to minimize test length while ensuring that uncertainties in latent factor estimation fall below a predefined threshold. We assess how many items each item selection algorithm requires before the posterior variance of each latent dimension of interest drops below  $\tau^2$ . In all experiments, we assume a zero-mean multivariate Gaussian prior with an identity covariance matrix and terminate the test when the posterior variance for all factors of interest satisfied  $\tau^2 < 0.16$  (equivalently, a posterior standard deviation  $\tau < 0.4$ ).

2. **Estimation Accuracy:** Beyond termination efficiency, it is essential to assess the rate of mean squared error (MSE) decay between the posterior mean and the oracle posterior mean. We define the oracle posterior as the posterior distribution obtained if test takers had answered all items in the item bank. In addition to comparing posterior means, we evaluate the full posterior distributions by examining their quantiles relative to the oracle posteriors.
3. **Computational Cost:** Given that CAT requires real-time interaction with test takers, we measure the online item selection time for each algorithm, particularly its efficiency in selecting a single item from a large item bank.

## 5.1 Simulations

We randomly generated a 5-factor, 200-item factor loading matrix  $B$  along with corresponding intercepts. The matrix  $B \in \mathbb{R}^{200 \times 5}$  was initially constructed by assigning each column a random permutation of 200 equally spaced values, with half sampled from  $[-0.9, -0.3]$  and the other half from  $[0.3, 0.9]$ , ensuring diverse loadings across dimensions while bounding the slope magnitudes by 3. To better reflect real-world datasets, where items rarely load on all five dimensions, each item was allowed to load on at most two factors. Additionally, the intercepts for each item were uniformly sampled from  $(-1.5, 1.5)$ .

In many CAT applications, the objective is to estimate only a subset of latent factors  $\mathcal{K} \in [K]$ , while treating the remaining factors as nuisance variables (as demonstrated in later sections with real data). To evaluate our approach in a challenging scenario, we focus on estimating the first three factors ( $\mathcal{K} = \{1, 2, 3\}$ ), while accounting for the presence of factors 4 and 5. Leveraging our proposed direct sampling approach outlined in Section 3, we implemented all CAT algorithms discussed in Sections 2 and 4. These include the Posterior Expected KL Information (EAP), the algorithm maximizing KL distance between successive posteriors (Max Pos), Mutual Information with posterior reweighting (MI), our proposed approach for maximizing prediction variances (Max Var) in Section 3.2, and the Q-learning approach.

For the Q-learning algorithm, we trained the Q-network as defined in Section 4.1 for 40,000 episodes. The exploration parameter  $\epsilon$  was decreased linearly from 0.99 to 0.01 over 750,000 steps. We set a sufficient large  $H = 70$  items, with discount factor  $\gamma = 0.95$ . To make sure the double Q-learning algorithm indeed converges to the optimal policy  $\pi^*$ , it is essential to make sure both the rewards and validation loss have stabilized. In Appendix D.1, we provide further details on the training dynamics of our deep Q-learning algorithm, illustrating the increase in rewards and the decrease in validation loss, both averaged over every 500 episodes throughout the training process.

To evaluate termination efficiency, we impose a standard zero-mean multivariate Gaus-

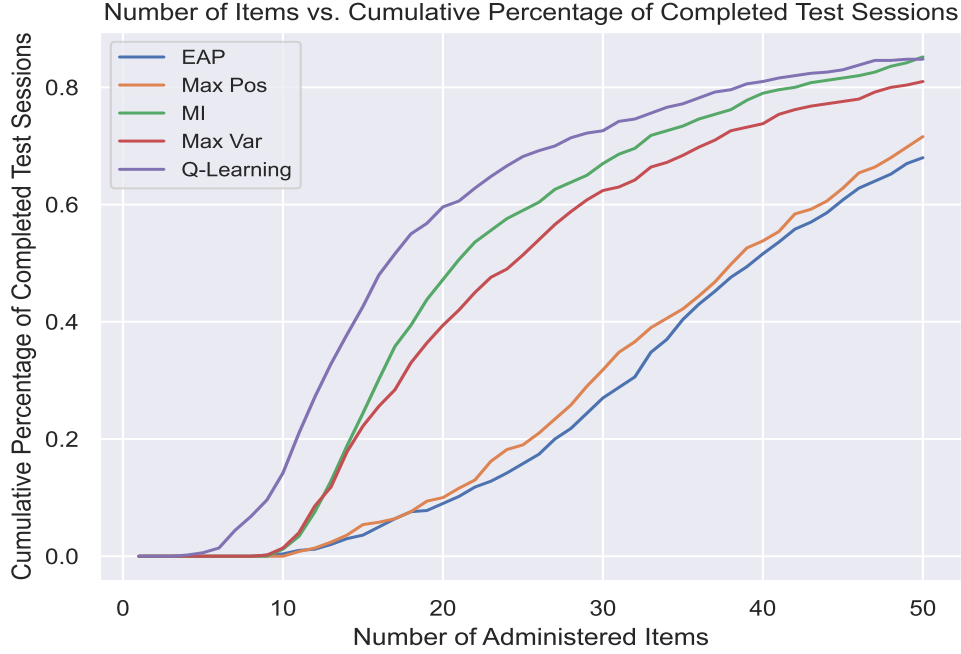


Figure 1: Number of Items Versus Cumulative Percentage of Completed Tests

Table 1: **Comparison of Winshares (W.S), Termination, and Computation**

Algorithm	Avg Termination (items)	W.S dim0	W.S dim1	W.S dim2	Avg Time (s/item)
EAP	37.6	17.6%	14.8%	11.6%	<b>0.025</b>
Max Pos	36.6	15.2%	13.4%	12.4%	0.028
MI	25.8	21.6%	20.2%	25.0%	0.084
Max Var	27.7	<b>23.0%</b>	24.4%	23.0%	0.036
Q-learning	<b>22.4</b>	22.6%	<b>27.2%</b>	<b>28.0%</b>	0.067

sian prior with an identity covariance matrix on the latent factors and dynamically terminate the test once the maximum posterior variance across all three target factors falls below  $\tau^2 < 0.16$  (posterior standard derivation  $\tau < 0.4$ ). Based on 500 simulated adaptive testing sessions, Figure 1 illustrates how the percentage of completed test sessions increases as more items are administered. Note that the test is considered completed only when all three factors have posterior variance below  $\tau^2$ . Faster growth rate of the completion percentages indicates faster variance reduction. Notably, the Mutual Information, Max Var, and Q-learning methods achieve significantly faster test termination compared to EAP and Max Pos. Among them, Q-learning exhibits the fastest variance reduction, as its reward function is explicitly designed to minimize posterior uncertainty. As summarized in the second column of Table 1, Q-learning requires an average of only 22.4 items to reach the termination criterion, outperforming all other methods.

Figure 2 illustrates how the mean squared error (MSE) between the posterior mean and the oracle posterior mean decreases as more items are administered. The MSE for



each latent dimension is averaged over 500 simulated adaptive sessions. Consistent with previous results, Q-learning, MI, and Max Var achieve significantly faster error reduction than EAP and Max Pos. While MSEs appear to converge after  $H = 20$  items, Q-learning exhibits a more rapid initial error reduction. To quantify this, we compute the MSE after 20 items for each of the 500 test sessions and determine win shares, defined as the percentage of test takers for whom each method achieves the lowest MSE after 20 items. These win shares are reported across all three latent dimensions (columns 3–5 in Table 1). Although MI, Max Var, and Q-learning all significantly outperform EAP and Max Pos, Q-learning achieves the lowest MSE in dimensions 1 and 2, while slightly trailing Max Var in dimension 0. Furthermore, all three methods provide better approximations of the full oracle distributions, extending beyond the posterior mean, as detailed in Appendix D.2.

The last column of Table 1 reports the average item selection time (in seconds) for each algorithm, highlighting the significant computational advantages of our direct sampling strategies. Among these, the EAP approach is the fastest, as it operates solely on one-dimensional response distributions. While Q-learning involves sampling from predictive distributions, it remains relatively fast due to the instantaneous computation of the feed-forward Q-network. Although we trained the Q-network using a single GPU, we emphasize that the 0.067-second online Q-learning item selection time was computed without GPU acceleration, demonstrating its accessibility on standard laptops. This experiment underscores the computational efficiency of our proposed methods in high-dimensional, large-item multivariate CAT settings. Notably, even the most computationally intensive mutual information approach requires only 0.084 seconds per item selection, as its computation benefits from our proposed posterior reweighting strategy.

## 5.2 Cognitive Function Measurements

We explore an important application of CAT algorithms for measuring cognitive function. Recently, pCAT-COG, the first computerized adaptive test based on MIRT for cognitive assessment, demonstrated CAT’s potential as an alternative to clinician-administered evaluations [7]. The item bank consists of  $J = 57$  items across five cognitive domains: episodic memory, working memory, executive function, semantic memory, and processing speed. This bank is being expanded to  $J = 500$  items for the full CAT-COG. Each item involves three tasks, scored on a scale from 0 to 3 based on the number of tasks answered correctly. For our analysis, we used a binary score, where 1 indicates correct answers on all tasks. After excluding examinees with missing responses, the final dataset included  $N = 730$  examinees.

Following the methodology in [7], we fit a six-factor bifactor model [34] (one primary factor and five subdomains) on the  $N$  by  $J$  binary responses, yielding a 57 by 6 factor loading matrix  $B$  and intercept vector  $D$ . In the bifactor model, each item loads on both

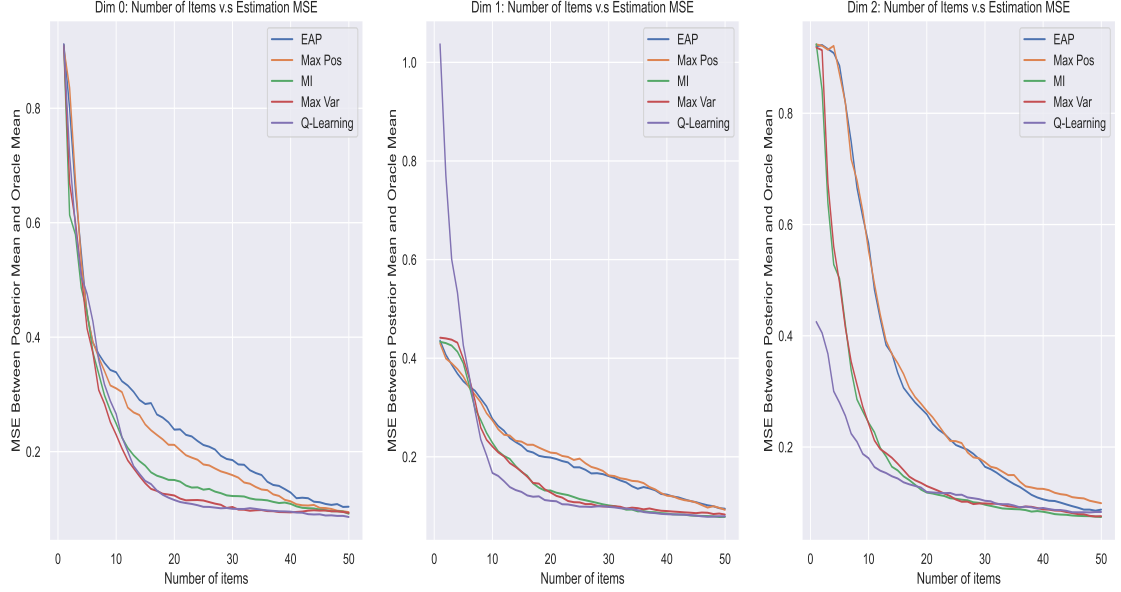


Figure 2: MSE Between Posterior Means and Oracle Posterior Means

the primary dimension and one of the five subdomains, as visualized in Figure 3. Given that pCAT-COG is designed to measure the global cognitive ability while accounting for multidimensional structure, we specified the Q-learning reward function to reduce posterior variance only for the primary factor, rather than minimizing global variance. The Q-network was trained offline for 40,000 episodes, with  $\epsilon$  decreasing linearly from 0.99 to 0.01 over 600,000 steps.

The experiment demonstrates the flexibility of our Q-learning algorithm, as the reward function can be tailored to meet specific research needs. While all the myopic policies discussed in Section 2.2 have desirable statistical properties, adapting these algorithms to prioritize the primary factor estimation was challenging. This is especially true in the bifactor model, where every item loads on the primary dimension, complicating item selection.

Since the Q-learning algorithm explicitly rewards variance reduction in the primary dimension, the left subplot of Figure 4 shows that it achieves significantly faster test termination compared to other methods. As before, we dynamically terminate the test when the posterior standard deviation drops below  $\tau = 0.4$ , and the cumulative percentage of completed test sessions is computed as the number of items administered increases. As shown in the first row of Table 2, Q-learning reached the desired posterior standard deviation threshold after an average of 11.1 items, while the MAX Pos approach required 19.8 items. Beyond variance reduction, the right subplot of Figure 4 highlights the rapid decay of mean squared error (MSE) in estimating the primary dimension with Q-learning,

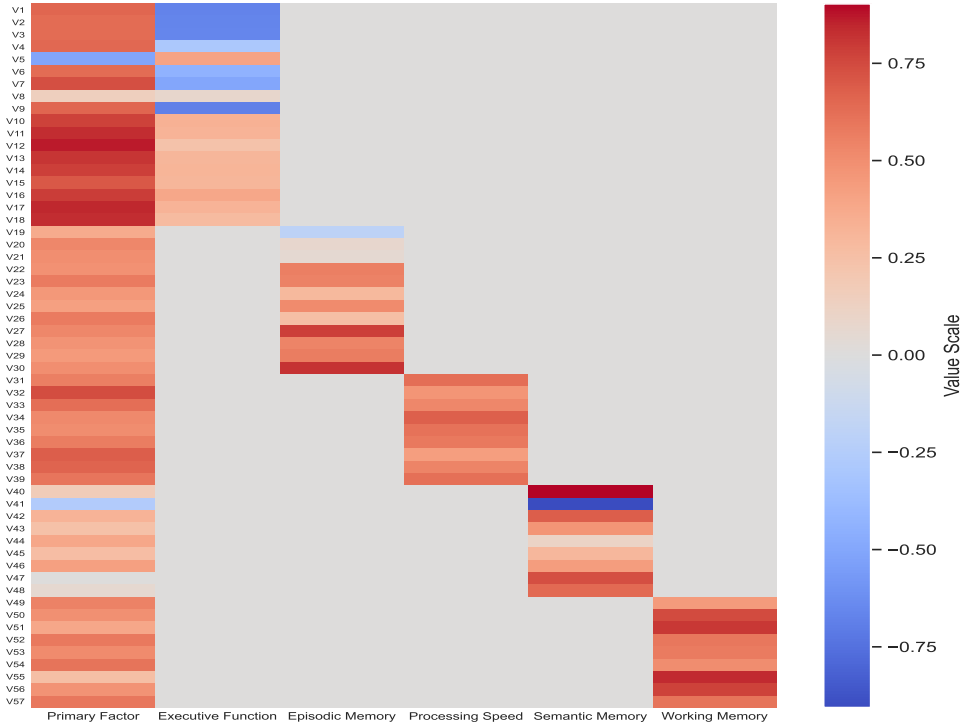


Figure 3: Estimated Bifactor Factor Loading Matrix for pCAT-COG

particularly in the early stages. As expected, MSE converged after about 30 items for all methods, since more than half of the item bank items had been administered.

To further compare algorithm performance, we consider adaptively selecting 20 items out of 57 for each test taker without dynamic termination and compare the resulting posteriors with the oracle posteriors (derived from all real item responses). We chose the number 20 because the MAX-POS approach required the largest average of 19.8 items for termination, and MSEs converged after 30 items for all algorithms, as shown in the right subplot of Figure 4. In particular, the second row of Table 2 shows that the Q-learning approach achieves the highest correlation of 0.958 between the estimated primary factor posterior means and the oracle posterior means after only 20 items. Additionally, the third row of Table 2 indicates that the Q-learning approach attains the highest win shares in estimating the primary dimension across all  $N = 730$  examinees. This is measured by computing the mean squared errors (MSE) between the posterior means obtained after administering  $H = 20$  adaptively selected items and the "true" posterior means derived from observing all  $J = 57$  items. For completeness, we also report the win shares for the other subdomains. Notably, Q-learning did not outperform all methods across all subdomains, as it was specifically designed to prioritize the primary dimension.

This experiment highlights the termination efficiency and estimation accuracy of our Q-learning algorithm in cognitive function measurement. Additionally, the flexibility of the algorithm allows for customized reward functions tailored to specific application needs.

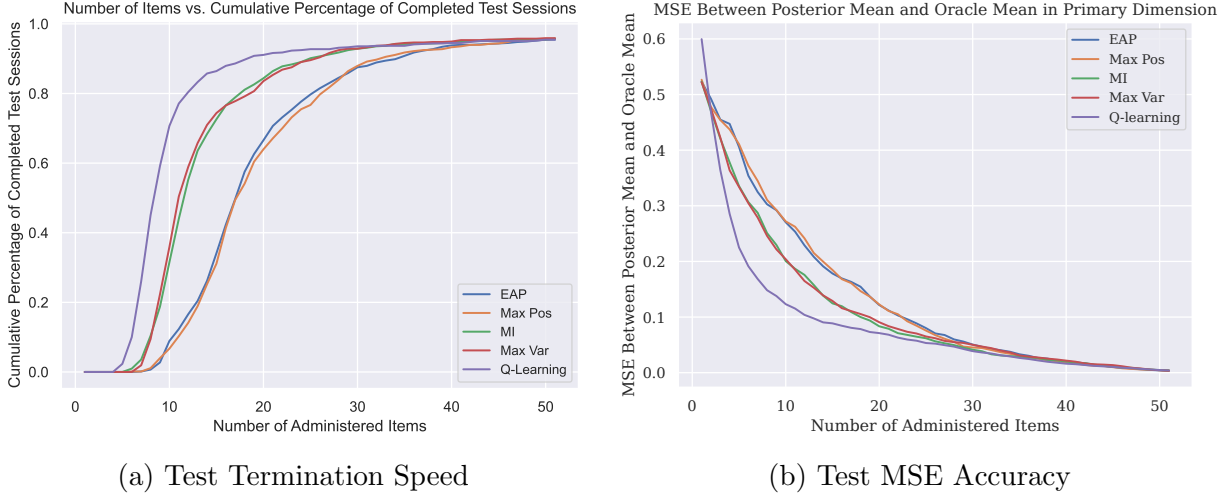


Figure 4: pCAT-COG: Primary Factor Posterior Variance Reduction (Left) and Estimation Accuracy (Right)

Table 2: Comparison of Winshares (W.S), Termination, and Computation

Metric	EAP	Max Pos	MI	Max Var	Q-Learning
Avg Termination (items)	19.5	19.8	14.4	14.2	<b>11.1</b>
Primary Factor Correlation	0.920	0.918	0.950	0.948	<b>0.958</b>
W.S Primary Factor	15.9%	15.9%	17.6%	20.7%	<b>29.9%</b>
W.S Executive Function	16.8%	17.1%	21.2%	19.6%	<b>25.3%</b>
W.S Episodic Memory	12.6%	14.9%	22.6%	<b>31.4%</b>	18.5%
W.S Processing Speed	15.2%	16.4%	20.7%	22.7%	<b>25.0%</b>
W.S Semantic Memory	11.4%	8.9%	<b>36.2%</b>	32.5%	11.0%
W.S Working Memory	17.0%	16.2%	20.5%	<b>23.3%</b>	23.0%
Avg Time (s/item)	<b>0.018</b>	0.019	0.028	0.020	0.031

We also demonstrate the advantages of our direct-sampling approach for Bayesian MCAT algorithms in high-dimensional latent space settings. Note that even for the computationally intensive mutual information method, our posterior reweighting strategy reduced item selection time to just 0.031 seconds for the six-dimensional item bank.

The pCAT-COG dataset also provides an ideal testbed for adaptive cognitive function assessments, as it presents a unique computational challenge of navigating a six-dimensional latent space in real time. The item selection algorithm must be computationally efficient to ensure seamless interactive testing, while also prioritizing the accurate measurement of the primary factor without neglecting subdomain influences. Unlike fixed test designs, online optimization is essential, as selecting an optimal sequence from 57 items is an inherently difficult combinatorial problem, even in a binary response setting. Moreover, the pCAT-COG item bank is currently being expanded to 500 items using a more nationally representative sample to improve racial and ethnic diversity. The success of our deep CAT framework on

this prototype dataset will demonstrate its scalability for larger-scale cognitive assessments, paving the way for broader deployment in clinical and research settings.

### 5.3 Educational Assessments

We consider an important application in educational assessment, utilizing 2022 Grade 8 student item response data from the Massachusetts Department of Elementary and Secondary Education (DESE). Excluding non-multiple-choice questions, the dataset includes responses from all Massachusetts Grade 8 students to 24 English items and 34 math items. For computational efficiency, we randomly sampled 1,000 student responses to evaluate each MCAT item selection algorithm. While [1] demonstrated the effectiveness of the PXL-EM algorithm in estimating interpretable factor loadings and the true number of factors using Grade 10 DESE data, we focus on Grade 8 due to its larger number of items.

Following the analysis in [1], we estimated item parameters via PXL-EM. The resulting factor loading matrix  $B$  is visualized in Figure 5, where dark blue regions indicate exact zeros. Notably, all English items load exclusively onto the first factor, representing general ability, while math items can also load onto factors 2–4, reflecting their greater structural complexity. For instance, the final factor ("Math 3") has nonzero loadings only on items 34, 36, and 38, all of which correspond to geometry problems.<sup>1</sup>

We focus on the problem of adaptively measuring the first factor while accounting for the underlying multidimensional structure. The left subplot of Figure 6 illustrates the cumulative percentage of completed test sessions for the 1,000 sampled examinees as more items are administered. As in previous experiments, the Q-learning algorithm exhibits the fastest variance reduction, significantly increasing the test completion rate. On average, Q-learning required only 20 items to reach the termination criterion, whereas the second-fastest method (MI) required nearly 26 items.

Beyond its efficiency in variance reduction, Q-learning also achieves a faster decay in MSE when estimating the first factor, reinforcing findings from earlier experiments. These results highlight the potential of Q-learning for educational assessments, demonstrating its ability to accelerate testing while maintaining accurate trait estimation.

## 6 Discussion

This work advocates for a deep reinforcement learning perspective in the design of multidimensional computerized adaptive testing (CAT) systems. We make two key contributions to the existing CAT literature: (1) a computational advancement that accelerates online item selection within a flexible Bayesian MIRT framework [1], and (2) a novel reinforcement

---

<sup>1</sup>Exam questions are available at: <https://www.doe.mass.edu/mcas/2022/release/>.

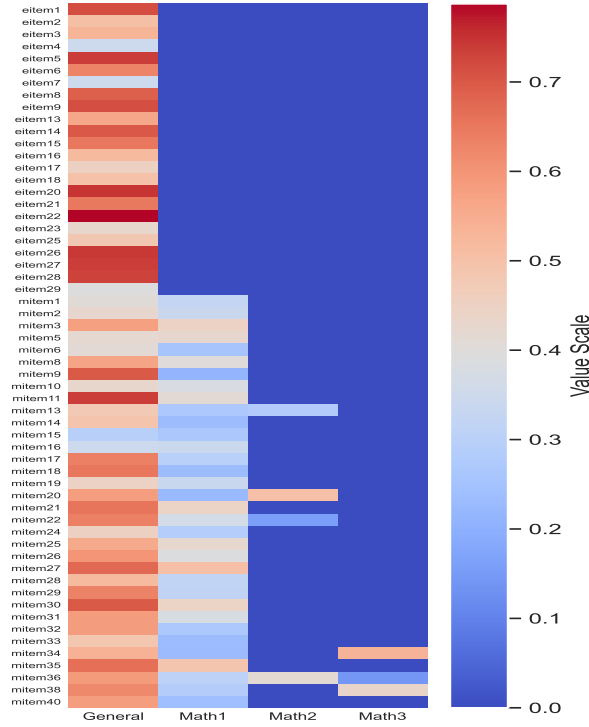


Figure 5: Estimated Factor Loadings for Grade 8 English and Math Items in Massachusetts (2022)

learning-based approach for conducting efficient adaptive testing.

First, we propose a computationally efficient direct sampling approach that eliminates the need for expensive MCMC sampling while imposing no strict factor loading constraints on the item bank. Our method is universally applicable to any existing CAT algorithm that requires sampling from latent factor posterior distributions, extending beyond the approaches discussed in Sections 2.2 and our proposed Q-learning framework. By leveraging direct sampling from unified skew-normal distributions, our methodology scales efficiently with a large number of factors and items, enabling near-instantaneous online item selection—even for computationally intensive objectives such as mutual information, when combined with posterior reweighting. Furthermore, this direct sampling strategy facilitates the construction of the prediction quartiles matrix  $\Psi_t$ , which enhances the Q-learning algorithm’s ability to effectively navigate the item bank environment.

The resulting computational gains provide greater flexibility in online item selection, a crucial factor in enhancing adaptive testing strategies. Unlike approaches that attempt to learn a fixed Bayesian test design offline [39], our framework enables fully dynamic item selection, allowing the test to adapt in real time and maximize the utilization of the item bank by exploring diverse testing trajectories. Furthermore, as demonstrated in Section 3.3, our method naturally extends to fully Bayesian item selection by incorporating uncertainty in item parameters, an essential consideration when the item bank is not well-calibrated.

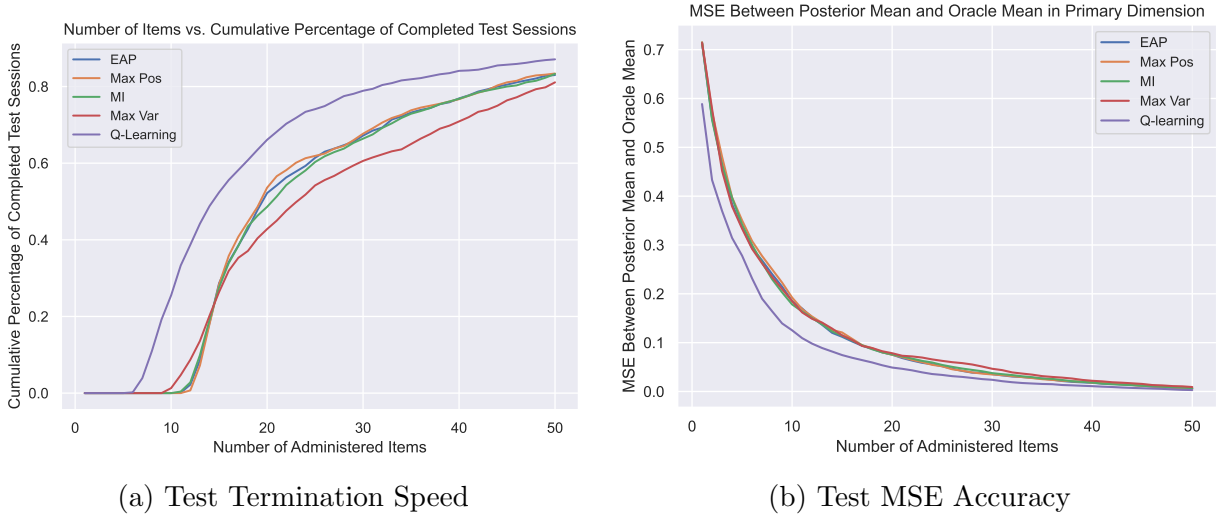


Figure 6: Educational Assessment: Main Factor Posterior Variance Reduction (Left) and Estimation Accuracy (Right)

The second major contribution of this work is the introduction of a deep double Q-learning algorithm for item selection, featuring a customized reward structure that directly targets posterior variance reduction. The offline-trained Q-network can be deployed efficiently online, enabling significantly faster test termination at a user-specified variance threshold. As demonstrated in both simulation and real-data studies, our Q-learning algorithm consistently achieves the fastest posterior variance reduction, which not only accelerates test termination but also reduces estimation bias, particularly in the early stages of testing. Moreover, because the Q-learning reward function can be tailored to accommodate different testing objectives, our approach provides a more principled and flexible framework for designing customized tests. These findings highlight the potential of reframing CAT as a reinforcement learning problem, where the goal is to learning an optimal policy that minimizing the test length, effectively addressing the myopic nature of traditional MCAT methods.

Our work also provides practical guidance for selecting the appropriate CAT item selection algorithm. The mutual information, maximizing prediction variance, and Q-learning approaches consistently outperform the EAP and the MAX Pos approaches across all evaluation criteria. The strong performance of the mutual information approach is expected, as it is well-established in the CAT literature [31, 6]. However, our proposed maximizing variance approach, while conceptually similar to mutual information (as discussed in Appendix A), offers significantly more efficient computation. For practitioners prioritizing data efficiency, fast dynamic termination, and error reduction, our deep Q-learning algorithm is the preferred choice. However, it requires additional offline training of the Q-network before deployment.

A promising direction for future work is to extend our methods to more general data



types, such as ordinal and categorical datasets. Recent work [1] shows that the latent factor posterior distribution under mixed binary and ordinal data retains the form of a degenerate unified skew-normal distribution. While this structure allows for efficient approximation, sampling from it remains challenging, potentially hindering rapid online selection. Developing more effective sampling schemes will be crucial to accommodating these broader data types.

Another exciting avenue is to explore alternative reward structures for our Q-learning algorithm. The flexibility of the Q-learning framework allows it to adapt to various reward specifications, particularly when the primary objective extends beyond fast dynamic termination. While the 0-1 reward structure is interpretable and stabilizes Q-network training, it provides sparse feedback, which may limit empirical performance. Alternative designs could incorporate intermediate rewards or increased penalization as more items are administered. A more theoretical yet challenging direction is to characterize when reinforcement learning approaches are particularly advantageous—or less effective—compared to myopic methods. This requires careful assumptions about the reward function and the item bank’s properties, providing deeper insights into the trade-offs between adaptive reinforcement learning and traditional item selection strategies.

## References

- [1] Jiguang Li, Robert Gibbons, and Veronika Rockova. Sparse bayesian multidimensional item response theory, 2024.
- [2] Wim J. van der Linden and Cees A. W. Glas. *Elements of Adaptive Testing*. Springer, New York, 2010.
- [3] Robert D. Gibbons, David J. Weiss, Ellen Frank, and David Kupfer. Computerized adaptive diagnosis and testing of mental health disorders. *Annual Review of Clinical Psychology*, 12:83–104, 2016. Epub 2015 Nov 20.
- [4] R.D. Bock and R.D. Gibbons. *Item Response Theory*. Wiley, 2021.
- [5] Alexander Weissman. Mutual information item selection in adaptive classification testing. *Educational and Psychological Measurement*, 67(1):41–58, 2007.
- [6] Joris Mulder and Wim Linden. *Multidimensional Adaptive Testing with Kullback–Leibler Information Item Selection*, pages 77–101. 01 2010.
- [7] Robert Gibbons, Diane Lauderdale, Robert Wilson, David Bennett, Tesnim Arar, and David Gallo. Adaptive measurement of cognitive function based on multidimensional

- item response theory. *Alzheimer's & Dementia: Translational Research & Clinical Interventions*, 10, 11 2024.
- [8] Daniel O. Segall. Multidimensional adaptive testing. *Psychometrika*, 61(2):331–354, 1996.
  - [9] Wim J. van der Linden. Multidimensional adaptive testing with a minimum error-variance criterion. *Journal of Educational and Behavioral Statistics*. Forthcoming, year unknown.
  - [10] Bernard Veldkamp and Wim Linden. Multidimensional adaptive testing with constraints on test content. *Psychometrika*, 67(4):575–588, December 2002.
  - [11] Hua-Hua Chang. Psychometrics behind computerized adaptive testing. *Psychometrika*, 80(1):1–20, March 2015.
  - [12] Hua-Hua Chang and Zhiliang Ying. a-stratified multistage computerized adaptive testing. *Applied Psychological Measurement*, 23(3):211–222, 1999.
  - [13] Richard S. Sutton and Andrew G. Barto. *Reinforcement Learning: An Introduction*. The MIT Press, second edition, 2018.
  - [14] Volodymyr Mnih, Koray Kavukcuoglu, David Silver, Andrei A. Rusu, Joel Veness, Marc G. Bellemare, Alex Graves, Martin Riedmiller, Andreas K. Fidjeland, Georg Ostrovski, Stig Petersen, Charles Beattie, Amir Sadik, Ioannis Antonoglou, Helen King, Dhharshan Kumaran, Daan Wierstra, Shane Legg, and Demis Hassabis. Human-level control through deep reinforcement learning. *Nature*, 518:529–533, 2015.
  - [15] Hado van Hasselt, Arthur Guez, and David Silver. Deep reinforcement learning with double q-learning. *Proceedings of the AAAI Conference on Artificial Intelligence*, 30(1), Mar. 2016.
  - [16] Reinaldo B. Arellano-Valle and Adelchi Azzalini. On the unification of families of skew-normal distributions. *Scandinavian Journal of Statistics*, 33(3):561–574, 2006.
  - [17] Daniele Durante. Conjugate bayes for probit regression via unified skew-normal distributions. *Biometrika*, 106(4):765–779, aug 2019.
  - [18] Z. I. Botev. The normal law under linear restrictions: Simulation and estimation via minimax tilting. *Journal of the Royal Statistical Society Series B: Statistical Methodology*, 79(1):125–148, feb 2016.

- [19] Dimitri P. Bertsekas and John N. Tsitsiklis. *Neuro-Dynamic Programming*. Athena Scientific, 1st edition, 1996.
- [20] David Silver, Aja Huang, Chris J. Maddison, Arthur Guez, Laurent Sifre, George Van Den Driessche, Julian Schrittwieser, Ioannis Antonoglou, Veda Panneershelvam, Marc Lanctot, Sander Dieleman, Dominik Grewe, John Nham, Nal Kalchbrenner, Ilya Sutskever, Timothy Lillicrap, Madeleine Leach, Koray Kavukcuoglu, Thore Graepel, and Demis Hassabis. Mastering the game of go with deep neural networks and tree search. *Nature*, 529(7587):484–489, 2016.
- [21] Dmitry Kalashnikov, Alex Irpan, Peter Pastor, Julian Ibarz, Alexander Herzog, Eric Jang, Deirdre Quillen, Ethan Holly, Mrinal Kalakrishnan, Vincent Vanhoucke, and Sergey Levine. Qt-opt: Scalable deep reinforcement learning for vision-based robotic manipulation. *ArXiv*, abs/1806.10293, 2018.
- [22] Xiao Li, Hanchen Xu, Jinming Zhang, and Hua hua Chang. Deep reinforcement learning for adaptive learning systems. *Journal of Educational and Behavioral Statistics*, 48(2):220–243, 2023.
- [23] Tom Rainforth, Adam Foster, Desi R. Ivanova, and Freddie Bickford Smith. Modern Bayesian Experimental Design. *Statistical Science*, 39(1):100 – 114, 2024.
- [24] Kathryn Chaloner and Isabella Verdinelli. Bayesian Experimental Design: A Review. *Statistical Science*, 10(3):273 – 304, 1995.
- [25] Paola Sebastiani and Henry P. Wynn. Maximum entropy sampling and optimal bayesian experimental design. *Journal of the Royal Statistical Society. Series B (Statistical Methodology)*, 62(1):145–157, 2000.
- [26] Adam Foster, Desi R. Ivanova, Ilyas Malik, and Tom Rainforth. Deep adaptive design: Amortizing sequential bayesian experimental design. In *International Conference on Machine Learning*, 2021.
- [27] Donald R Jones, Matthias Schonlau, and William J Welch. Efficient global optimization of expensive black-box functions. *Journal of Global Optimization*, 13(4):455–492, 1998.
- [28] Niranjana Srinivas, Andreas Krause, Sham M Kakade, and Matthias W Seeger. Gaussian process optimization in the bandit setting: No regret and experimental design. In *Proceedings of the 27th International Conference on Machine Learning (ICML)*, pages 1015–1022. Omnipress, 2010.

- [29] Philipp Hennig and Christian J. Schuler. Entropy search for information-efficient global optimization. *Journal of Machine Learning Research*, 13:1809–1837, 2012.
- [30] Remi Lam, Karen Willcox, and David H. Wolpert. Bayesian optimization with a finite budget: An approximate dynamic programming approach. In D. Lee, M. Sugiyama, U. Luxburg, I. Guyon, and R. Garnett, editors, *Advances in Neural Information Processing Systems*, volume 29. Curran Associates, Inc., 2016.
- [31] Chun Wang and Hua-hua Chang. Item selection in multidimensional computerized adaptive testing—gaining information from different angles. *Psychometrika*, 76(3):363–384, 07 2011. Copyright - The Psychometric Society 2011; Last updated - 2023-12-03.
- [32] Ying Cheng and Hua-Hua Chang. The maximum priority index method for severely constrained item selection in computerized adaptive testing. *British Journal of Mathematical and Statistical Psychology*, 62(2):369–383, 2009.
- [33] Alfréd Rényi. On measures of entropy and information. 1961.
- [34] Robert D. Gibbons and Donald Hedeker. Full-information item bi-factor analysis. *Psychometrika*, 57(3):423–436, September 1992.
- [35] A. F. M. Smith and A. E. Gelfand. Bayesian statistics without tears: A sampling-resampling perspective. *The American Statistician*, 46(2):84–88, 1992.
- [36] Wim J. van der Linden and Hao Ren. A fast and simple algorithm for bayesian adaptive testing. *Journal of Educational and Behavioral Statistics*, 45(1):58–85, 2020.
- [37] Manzil Zaheer, Satwik Kottur, Siamak Ravanbakhsh, Barnabás Póczos, Ruslan Salakhutdinov, and Alexander J Smola. Deep sets. In *Proceedings of the 31st International Conference on Neural Information Processing Systems*, NIPS’17, page 3394–3404, Red Hook, NY, USA, 2017. Curran Associates Inc.
- [38] Carri W. Chan and Vivek F. Farias. Stochastic depletion problems: Effective myopic policies for a class of dynamic optimization problems. *Mathematics of Operations Research*, 34(2):333–350, 2009.
- [39] Chelsea Krantsevich, P. Richard Hahn, Yi Zheng, and Charles Katz. Bayesian decision theory for tree-based adaptive screening tests with an application to youth delinquency. *Annals of Applied Statistics*, 17(2):1038–1063, June 2023.

# Supplementary Material: Deep Computerized Adaptive Testing

## A Mutual Information as Prediction Uncertainties

We observe all the heuristic Bayesian item selection methods discussed in this manuscript account for prediction uncertainty. In particular, the mutual information item selection rule can be rewritten as follows:

$$\begin{aligned}
 \arg \max_{j_t \in R_t} I_M(\theta, y_{j_t}) &= \arg \max_{j_t \in R_t} \sum_{y_{j_t}=0}^1 \int_{\theta} f(\theta, y_{j_t} | Y_{t-1}) \log \frac{f(\theta, y_{j_t} | Y_{t-1})}{f(\theta | Y_{t-1}) f(y_{j_t} | Y_{t-1})} d\theta \\
 &= \arg \max_{j_t \in R_t} \sum_{y_{j_t}=0}^1 \int_{\theta} f(y_{j_t} | \theta) f(\theta | Y_{t-1}) \log \frac{f(\theta, y_{j_t} | Y_{t-1})}{f(\theta | Y_{t-1}) f(y_{j_t} | Y_{t-1})} d\theta \\
 &= \arg \max_{j_t \in R_t} \sum_{y_{j_t}=0}^1 \int_{\theta} f(y_{j_t} | \theta) f(\theta | Y_{t-1}) \log \frac{f(y_{j_t} | \theta)}{f(y_{j_t} | Y_{t-1})} d\theta \\
 &= \arg \max_{j_t \in R_t} \int_{\theta} [\Phi(B'_{j_t} \theta + d_{j_t}) \log \frac{\Phi(B'_{j_t} \theta + d_{j_t})}{c_{j_t}} + \\
 &\quad (1 - \Phi(B'_{j_t} \theta + d_{j_t})) \log \frac{(1 - \Phi(B'_{j_t} \theta + d_{j_t}))}{(1 - c_{j_t})}] f(\theta | Y_{t-1}) d\theta.
 \end{aligned} \tag{19}$$

Equation (19) suggests the mutual information criterion selects the item  $j_t$  that has the largest expected KL divergence between the Bernoulli distributions parametrized by  $\Phi(B'_{j_t} \theta + d_{j_t})$  and  $c_{j_t}$ , weighted by the current posterior  $f(\theta | Y_{t-1})$ .

Observe that mutual information essentially favors the item  $j_t$  that has the largest prediction uncertainties around its prediction mean  $c_{j_t}$ , quantified by the KL divergence. To compare equation (19) with equation (13), note we have replace the integral of KL divergence from  $c_{j_t}$  with variances  $(\Phi(B'_{j_t} \theta + d_{j_t}) - c_{j_t})^2$  in (13). This suggests that our proposed approach shares similar theoretical properties with the mutual information criterion, but offers a much simpler formula for online computation, avoiding posterior reweighting and log transformations. Empirically, our proposed item selection rule achieves comparable performance to mutual information but with significantly reduced computational time.

## B Fully Bayesian Item Selection Simulation

We evaluate the effectiveness of our direct sampling approach in enabling fully Bayesian online item selection. Unlike traditional methods that treat item parameters as fixed, the

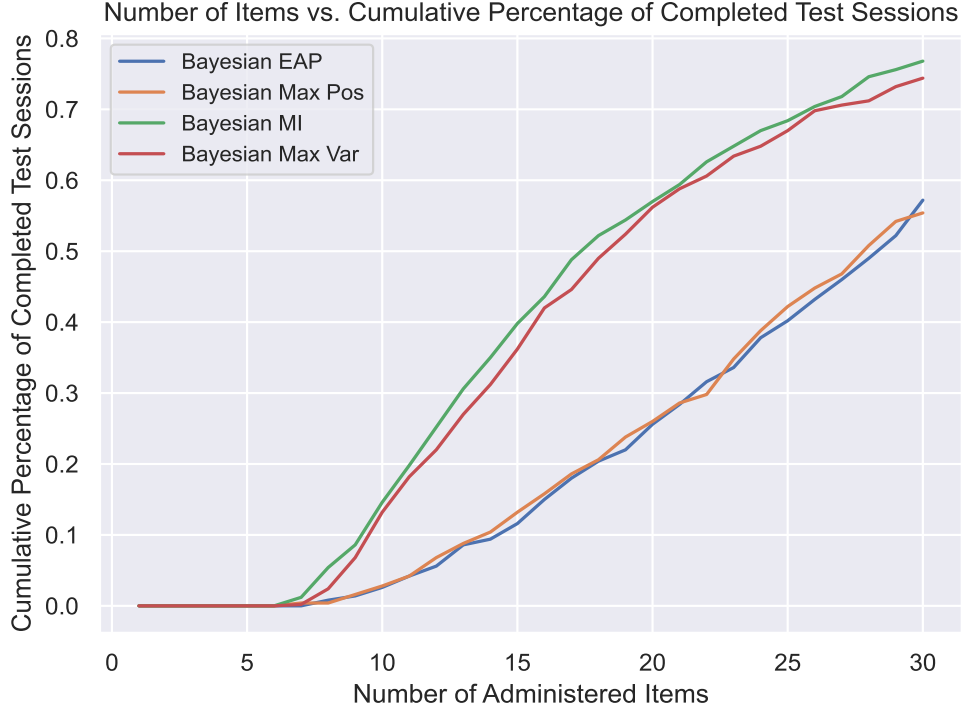


Figure 7: Fully Bayesian: Number of Items Versus Posterior Variance Reduction

fully Bayesian approach explicitly accounts for their uncertainties, which can be substantial when the item response dataset is small or poorly calibrated. To illustrate, we generate a binary item response dataset  $Y$  with  $N = 500$  examinees and  $J = 150$  items under a 3-factor probit MIRT model. The true factor loading matrix  $B$  has dimensions  $J \times 3$ , and the intercept vector  $D$  has 150 elements.

To integrate item parameter uncertainty into online item selection, we fit a Gibbs sampler to the  $N \times J$  item response data. We generated 5,000 MCMC draws, retaining the last 500 posterior samples of the item parameters  $\Xi = \xi^{(m)}_{m=1}^{500}$  after burn-in. As described in Section 3.3, the fully Bayesian approach marginalizes over the joint distributions of the nuisance item parameters  $\Xi$  and latent traits. We then implemented all item selection rules depicted in Sections 2.2 and 3.2 in a fully Bayesian manner.

Figure 7 illustrates the cumulative percentage of completed test sessions across all 500 simulated examinees as more items are administered. The test was dynamically terminated when the posterior standard deviations across all three factors fell below 0.4. Consistent with the experimental results in Section 5 of the manuscript, the mutual information method and our proposed Max Var method demonstrated superior posterior variance reduction. The second column of Table 3 shows that the mutual information method terminated after an average of 18.7 items, whereas the EAP approach required 24.4 items.

Beyond variance reduction, the mutual information and maximizing prediction variance

Table 3: Comparison of Winshares (W.S), Termination, and Computation

Algorithm	Avg Termination (items)	W.S dim0	W.S dim1	W.S dim2	Avg Time (s/item)
EAP	24.4	22.2%	19.2%	21.8%	4.10
Max Pos	24.2	17.4%	18.0%	21.0%	4.10
MI	<b>18.7</b>	<b>32.8%</b>	31.0%	27.8%	4.11
Max Var	19.2	27.6%	<b>31.8%</b>	<b>29.4%</b>	4.10

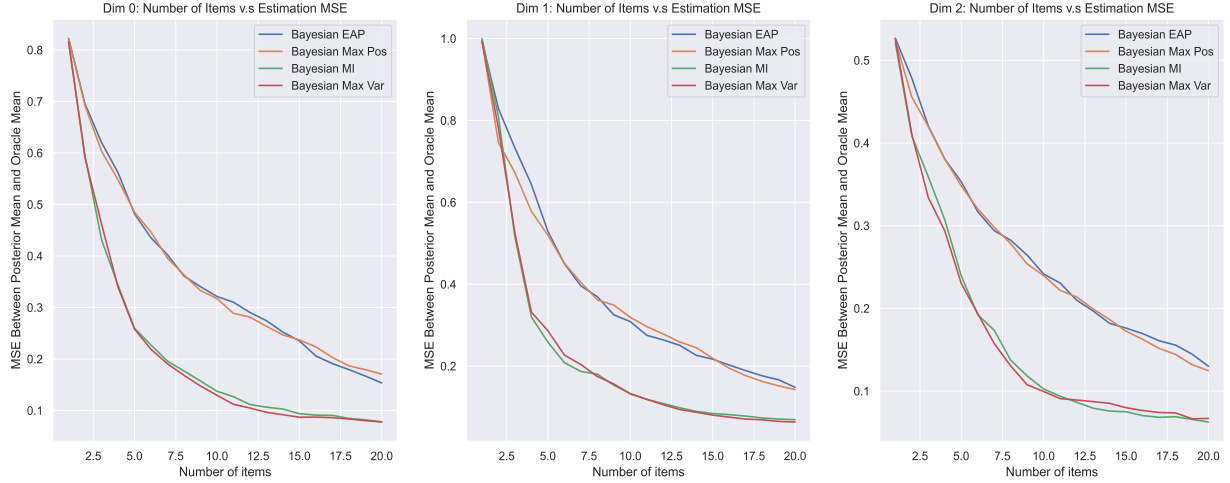


Figure 8: Fully Bayesian: MSE Between Posterior Mean and Oracle Posterior Mean

methods also exhibited superior estimation accuracy, as shown in Figure 8, which tracks the decline in mean squared error (MSE) between the posterior mean and the oracle posterior mean. Since estimation errors stabilized around  $H = 30$  items, we compared MSEs between the posterior mean at  $H = 20$  and the oracle posterior mean, and then summarized the win shares for each item selection rule across all 500 examinees and all three dimensions in Table 3.

Finally, we emphasize that even in a fully Bayesian framework, where nuisance parameters are integrated rather than fixed, our approach remains computationally efficient. Across all item selection rules, online selection required an average of just 4.1 seconds per test session on a personal laptop, highlighting the scalability of our direct sampling method for Bayesian MCAT applications. Readers may notice that 4.1 seconds is significantly longer than the item selection time reported in the experimentation section, where item parameters are treated as fixed. This discrepancy arises because fully Bayesian MCAT requires sampling from  $M = 500$  distinct unified-skew normal distributions for each item selection, whereas the standard case involves sampling from a single fixed distribution. This also explains the minimal differences in item selection time across algorithms, as the primary computational bottleneck lies in sampling from these distributions. When more CPUs are available, we can certainly sampling from all  $M$  distributions in parallel, and



hence further improving the 4.1 seconds benchmark.

## C Proof of Theorem 4.1

*Proof.* We proceed by induction. Since the myopic and the optimal policy would agree on time  $t = H - 1$ , the inequality holds trivially for the base case. For the induction step, we assume the claimed inequality holds for all  $t'$  such that  $H > t' > t$ . Consider the time horizon  $t < t'$  and let  $a_1$  represent the item chosen by the optimal policy and  $a_2$  the item chosen by the myopic policy. The inequality holds trivially for  $a_1 = a_2$ . Hence, we consider the case when  $a_1 \neq a_2$  and let  $y_{a_1}$  and  $y_{a_2}$  represent the binary random variables for the item response. For given extended state  $\bar{s}$ , we have

$$\begin{aligned} V_{\pi^*}(\bar{s}|y_{a_1}, y_{a_2}) &= E[R(\bar{s}, a_1, \bar{s}')|y_{a_1}] + V_{\pi^*}(\hat{G}_{y_{a_1}}(\bar{s})) \\ &\leq E[R(\bar{s}, a_1, \bar{s}')|y_{a_1}] + E[R(\bar{s}, a_2, \bar{s}')|y_{a_2}] + V_{\pi^*}(\tilde{G}_{y_{a_2}}(\hat{G}_{y_{a_1}}(\bar{s}))) \end{aligned} \quad (20)$$

$$\begin{aligned} &= E[R(\bar{s}, a_1, \bar{s}')|y_{a_1}] + E[R(\bar{s}, a_2, \bar{s}')|y_{a_2}] + V_{\pi^*}(\hat{G}_{y_{a_1}}(\tilde{G}_{y_{a_2}}(\bar{s}))) \\ &\leq E[R(\bar{s}, a_1, \bar{s}')|y_{a_1}] + E[R(\bar{s}, a_2, \bar{s}')|y_{a_2}] + V_{\pi^*}(\hat{G}_{y_{a_2}}(\bar{s}))) \end{aligned} \quad (21)$$

$$\leq E[R(\bar{s}, a_1, \bar{s}')|y_{a_1}] + E[R(\bar{s}, a_2, \bar{s}')|y_{a_2}] + 2V_{\pi^m}(\hat{G}_{y_{a_2}}(\bar{s}))). \quad (22)$$

Note we applied the immediate rewards assumption in equation (20), the value function monotonicity assumption in equation (21), and the induction hypothesis in equation (22). Now, we may take expectation over  $y_{a_1}$  and  $y_{a_2}$  on both side of inequality and obtain:

$$\begin{aligned} V_{\pi^*}(\bar{s}) &\leq E[R(\bar{s}, a_1, \bar{s}')] + E[R(\bar{s}, a_2, \bar{s}')] + 2V_{\pi^m}(\hat{G}_{y_{a_2}}(\bar{s}))) \\ &\leq 2(E[R(\bar{s}, a_2, \bar{s}')] + V_{\pi^m}(\hat{G}_{y_{a_2}}(\bar{s}))) = 2V_{\pi^m}(\bar{s}). \end{aligned}$$

The last inequality is due to the fact the  $\pi^m$  is the myopic policy that maximizes the next step reward.  $\square$

## D More Analysis on Simulation

### D.1 Double Q-Learning Training Dynamics

In Figure 9, we present two key metrics illustrating the training dynamics of our Q-learning algorithm. The left subplot displays the average episode rewards, computed over every 500 training episodes, showing that rewards began converging around episode 20,000 at approximately  $-25$ . The right subplot shows the average validation loss, also computed over every 500 episodes, indicating convergence around a loss value of 2. Given that



Figure 9: Training Dynamics for the Simulation Experiment in Section 5.1

$H = 70$  in this experiment, the reward is bounded within  $[-70, 1]$ , and the observed MSE of 2 between the primary and target network suggests good convergence.

Since we save the primary neural network every 500 episodes, we select the checkpoint corresponding to the highest average reward for offline deployment in future item selection tasks. In this case, the network at episode 35,000 is chosen, as it achieves the peak average reward of approximately  $-24.4$ . This model selection strategy is consistently applied across all experiments in Section 5.

## D.2 Matching the Oracle Posterior

Recall the "oracle posterior distribution" of a test taker is defined as the posterior obtained if the given test taker had answered all items in the item bank. To obtain the oracle distributions for each of the 500 test taker in Section 5.1, we simulate their item response to all 200 items in the test bank, and then calculate the posterior distribution using Theorem 3.2.

Figures 10, 11, and 12 illustrate the decrease of the estimation MSE for the first quartile, median, and the third quartiles compared to those of the oracle distribution, respectively. The quartiles of each posterior distribution is computed via 1,000 independent draws. In all these figures, we observe similar superior performances for the MI, Max Var, and the Q-learning methods over the EAP and the MAX pos approaches in estimating the entire

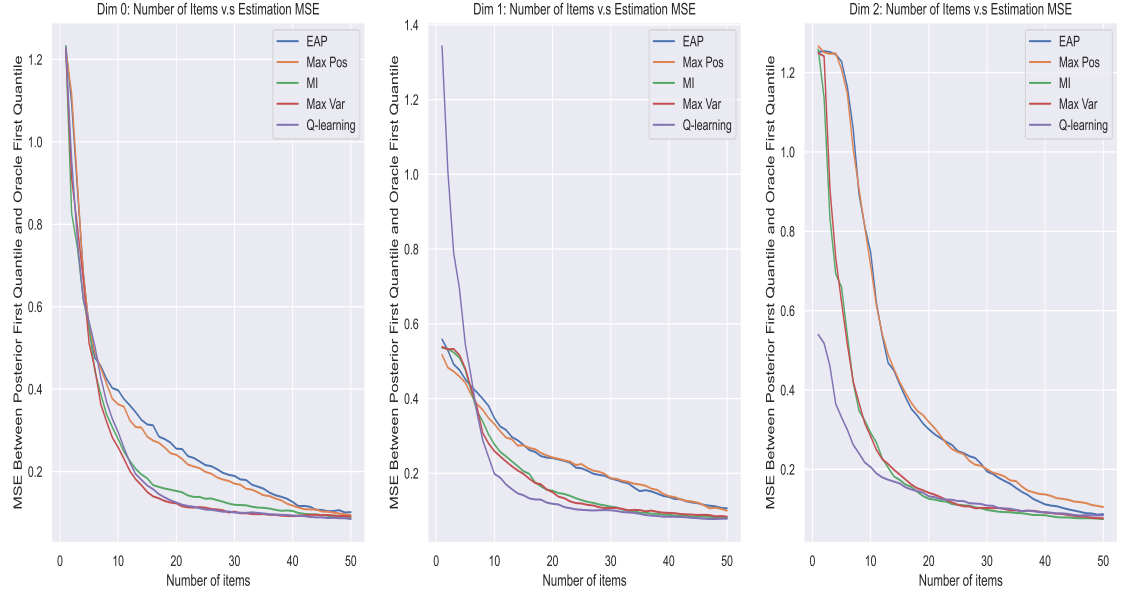


Figure 10: MSE Between Posterior 1st Quantile and Oracle 1st Quantile

oracle distributions. Consistent with the findings in Section 5.1, the Q-learning approach demonstrates the fastest error reduction rate, especially in the early stages of the test.

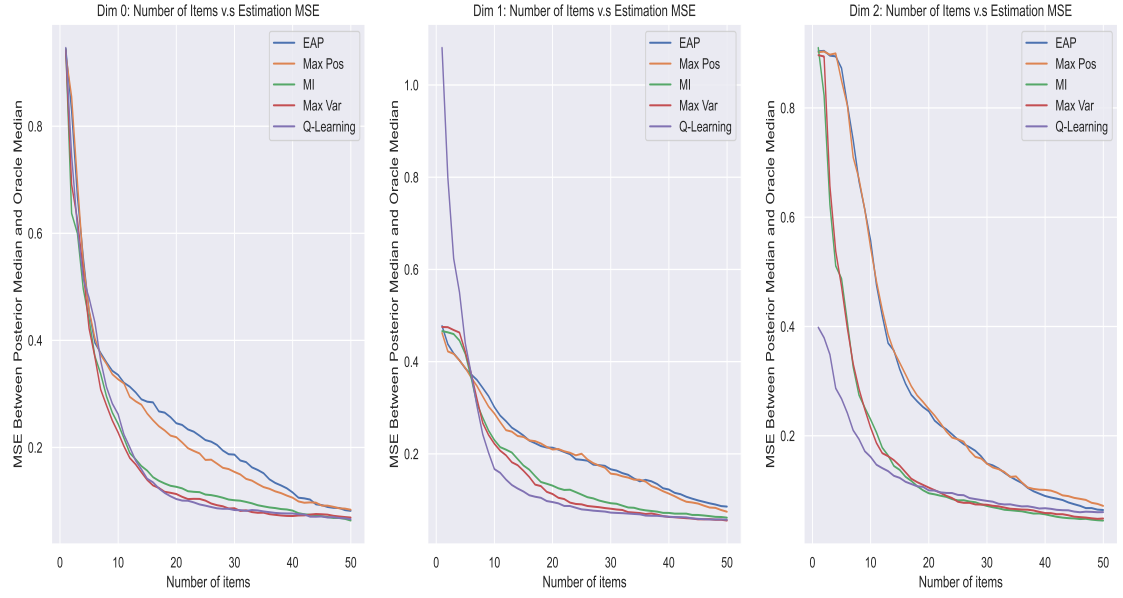


Figure 11: MSE Between Posterior Median and Oracle Median

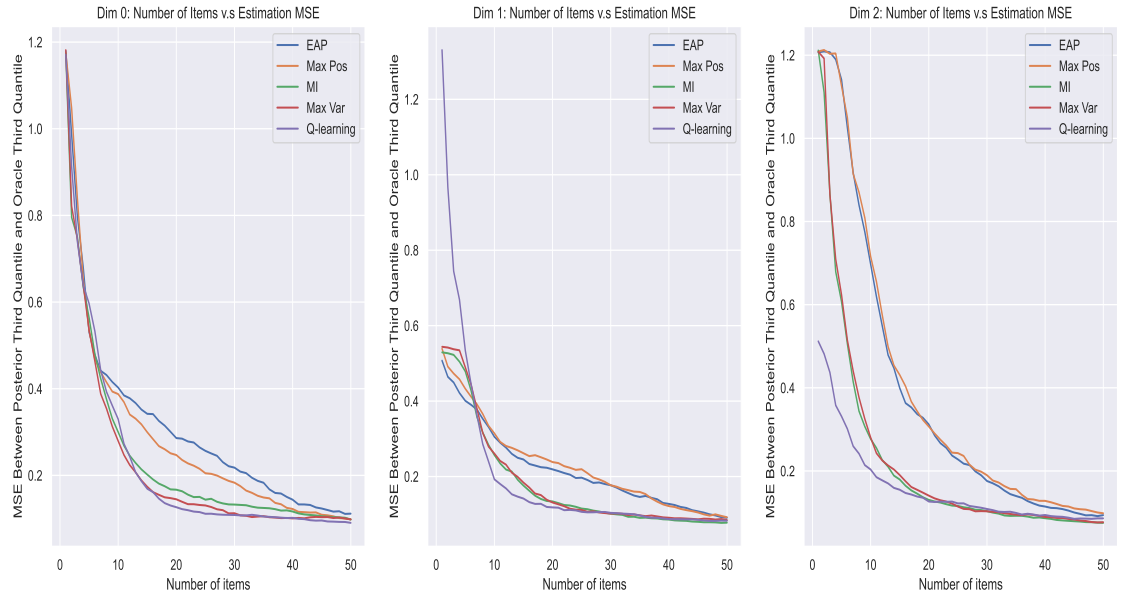


Figure 12: MSE Between Posterior 3rd Quantile and Oracle 3rd Quantile